5-21-2019

ACC Theta Improves Hippocampal Contextual Processing during Remote Recall

Ryan A. Wirt
University of Nevada, Las Vegas, ryan.wirt@unlv.edu

James M. Hyman
University of Nevada, Las Vegas, james.hyman@unlv.edu

Repository Citation

Wirt, R. A., Hyman, J. M. (2019). ACC Theta Improves Hippocampal Contextual Processing during Remote Recall. *Cell Reports, 27*(8), 2313-2327. Elsevier.
http://dx.doi.org/10.1016/j.celrep.2019.04.080

Article

Cell Reports

ACC Theta Improves Hippocampal Contextual Processing during Remote Recall

Graphical Abstract

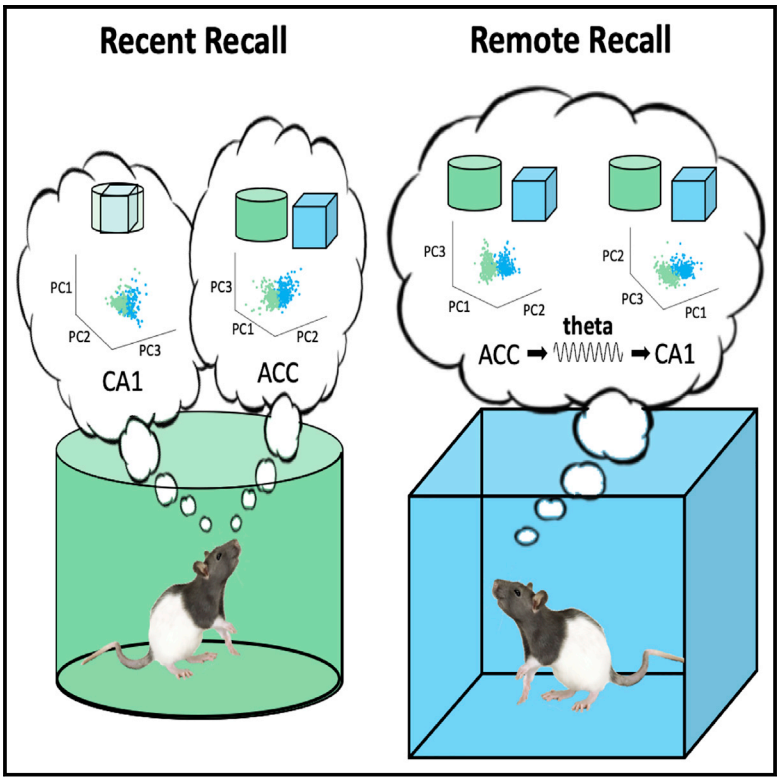

Authors

Ryan A. Wirt, James M. Hyman

Correspondence

james.hyman@unlv.edu

In Brief

Over time, contextual memories become dependent on the ACC for retrieval. Wirt and Hyman found that theta-mediated interactions between ACC and CA1 increase for remote recall. Communication from the ACC to CA1 modulates neural oscillations and unit spiking, leading to enhanced CA1 contextual information.

Highlights

- ACC leads CA1 during remote recall
- ACC theta modulates CA1 spiking and gamma power during remote recall
- ACC and CA1 ensemble context information increases over consolidation
- Consolidation increases the strength and spread of ACC theta effects on CA1 networks

Wirt & Hyman, 2019, Cell Reports *27*, 2313–2327
May 21, 2019
https://doi.org/10.1016/j.celrep.2019.04.080

CellPress

Cell Reports
Article

ACC Theta Improves Hippocampal Contextual Processing during Remote Recall

Ryan A. Wirt[1] and James M. Hyman[1,2,*]
[1]Department of Psychology, University of Nevada Las Vegas, 4505 S. Maryland Parkway, MS 5030, Las Vegas, NV 89154, USA
[2]Lead Contact
*Correspondence: james.hyman@unlv.edu
https://doi.org/10.1016/j.celrep.2019.04.080

SUMMARY

Consolidation studies show that, over time, memory recall becomes independent of the medial temporal lobes. Multiple lines of research show that the medial frontal cortex, including the anterior cingulate cortex (ACC), is involved with contextual information processing and remote recall. We hypothesize that interactions between the ACC and hippocampal area CA1 will change as memories became more remote. Animals are re-exposed to multiple environments at different retention intervals. During remote recall, ACC-CA1 theta coherence increases, with the ACC leading area CA1. ACC theta regulates unit spike timing, gamma oscillations, and ensemble and single-neuron information coding in CA1. Over the course of consolidation, the strength and prevalence of ACC theta modulation grow, leading to richer environmental context representations in CA1. These data are consistent with the transference of contextual memory dependence to the ACC and indicate that remote memories are retrieved via ACC-driven oscillatory coupling with CA1.

INTRODUCTION

Few neural processes are as important to survival as contextual memory formation and retrieval. The ability to associate a context with stimuli and events is essential for evading predation and other dangerous situations, foraging, hunting, and social interaction. In some way every one of these behavioral processes is contingent upon one's milieu. Contextual memory information is dependent on the hippocampus (HC) during initial encoding and for successful memory recall in the days following (recent recall; Scoville and Milner, 1957; Squire and Alvarez, 1995; Squire et al., 2001; Varela et al., 2016). However, after enough time has passed from encoding (i.e., remote recall), the HC is no longer needed for successful memory retrieval (McClelland et al., 1995; Maviel et al., 2004; Frankland et al., 2006). This process whereby memory dependence is transferred from the HC to other neural areas for long-term storage is known as consolidation (McGaugh, 2000; Dudai, 2004). Although there is still great debate about this process (i.e., standard consolidation model, standard consolidation model with schemas, multiple trace hypothesis), much data have shown that the ability to retrieve memories is dependent on different neural areas as time passes (for review, see Squire et al., 2015).

Memories are thought to be stored as a loose connection of distributed networks spread out in many brain regions, with individual features reliant on different areas (Mishkin, 1982; Rissman and Wagner, 2012). For instance, visual information is stored in visual areas (Mishkin, 1979), auditory in auditory areas (Alain et al., 1998), olfactory in olfactory areas (Slotnick et al., 1991), fear in the amygdala (Phelps et al., 1998), and reward in the ventral tegmental area (VTA; Adcock et al., 2006) and orbital frontal cortex (Rolls, 2000). Contextual information is unique because it is by definition more global than these other examples, encompassing both local and distal spatial cues, along with emotional, cognitive, social, and behavioral information.

The medial frontal cortex, particularly the anterior cingulate cortex (ACC), is integral for processing global contextual information (Devinsky et al., 1995). In humans, the ACC is linked with many different types of context representations, including task context (Paus et al., 1998), social context (Amodio and Frith, 2006), and environmental context (Walton and Mars, 2007). Similarly, in animal models ACC neurons encode the where (Hyman et al., 2012; Rozeske et al., 2015), when (Ma et al., 2014), what (Weible et al., 2009), how (Durstewitz et al., 2010), and emotional (Vetere et al., 2011) aspects of contextual representations (for review, see Wirt and Hyman, 2017). Importantly, these findings extend into memory retrieval, showing that as time passes the ACC's role in contextual processing increases (Teixeira et al., 2006). This is true for both appetitive (Frankland et al., 2004) and aversive (Takehara-Nishiuchi and McNaughton, 2008) tasks. Successful remote recall is dependent on the ACC being intact and leads to increases in the amounts of several biomarkers indicative of neural activity (Maviel et al., 2004; Takehara-Nishiuchi and McNaughton, 2008). For example, Bontempi et al. (1999) found that cFos activation in the ACC markedly increased during remote but not recent contextual recall. Interestingly, in the same study the opposite effects were detected for hippocampal area CA1, suggesting that as time passes contextual memory dependence is transferred from the HC to the ACC.

Separately, there is a rich literature showing that interactions between these same two areas are integrally important for working memory performance (Jones and Wilson, 2005; Hyman et al., 2010; Benchenane et al., 2010; Westendorff et al., 2016). Strong interactions occur primarily around the hippocampal theta oscillation (7–12 Hz), and such effects can be seen in theta coherence (Myroshnychenko et al., 2017), entrainment of unit activity

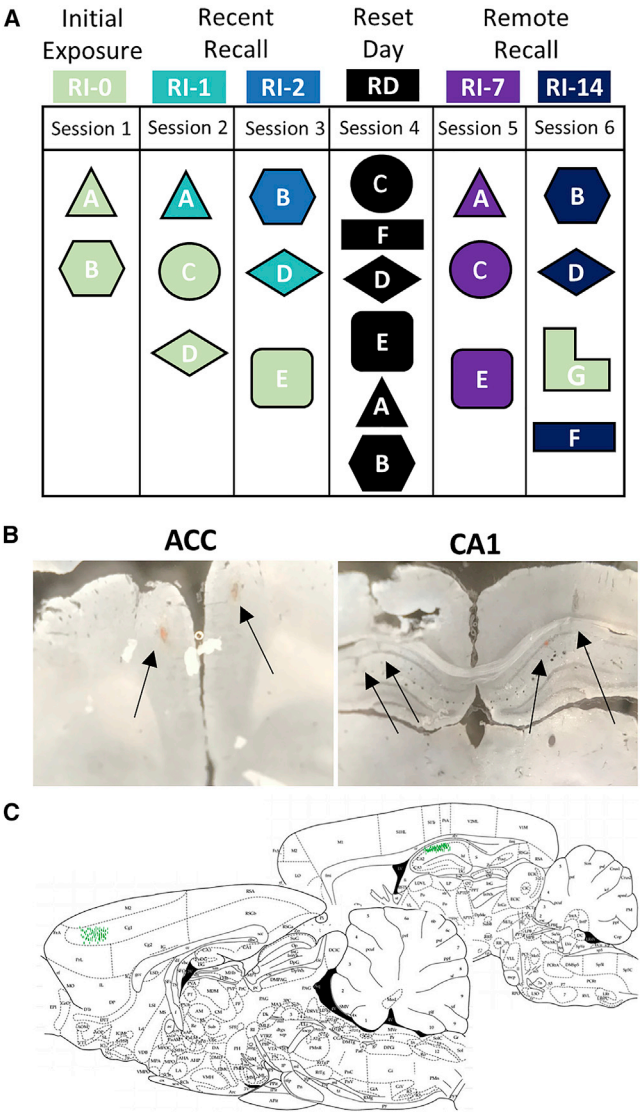

Figure 1. Behavioral Task and Verification of Tetrode Placement

(A) Schematic of behavioral protocol. Subjects were introduced into seven novel environments and then re-introduced at differing delay periods. Different colors represent retention intervals: green (RI-0) represents initial exposure, teal (RI-1) and blue (RI-2) represent recent recall, and purple (RI-7) and dark blue (RI-14) represent remote recall. Session 4, shown in black (RD), was a behavioral reset day to control for time from last visit and is not included in any of the analyses.

(B) Recording locations. Representative examples of ACC (left) and CA1 (right) recording tracks.

(C) Schematic of all recording locations in the ACC (left) and CA1 (right).

(Siapas et al., 2005; Hyman et al., 2005, 2010; Jones and Wilson, 2005; O'Neill et al., 2013), or cross-frequency coupling (Sirota et al., 2008; Tamura et al., 2017). In fact, Hallock et al. (2016) showed that merely impairing theta interactions between these areas was sufficient to compromise working memory. However, no studies have yet shown similar interactions occurring during remote memory recall.

For the present study, we set out to determine whether the electrophysiological markers of ACC-CA1 interactions changed as memories matured. Investigating this possibility required a task in which behavior was both consistent and distinct over sessions. Cognitive processes and motor activity have profound impacts on electrophysiological activity in both areas (oscillatory frequency and power: Pickenhain and Klingberg, 1967; Vanderwolf, 1969; Vanderwolf et al., 1973; oscillatory interactions: Siapas et al., 2005; Benchenane et al., 2010; Sigurdsson et al., 2010; unit-oscillatory interactions: Jones and Wilson, 2005; Hyman et al., 2005; 2010; Ito et al., 2015; and unit information coding: Hyman et al., 2005; Ma et al., 2016). In turn, these markers are influenced by a diverse array of factors, including behavioral-cognitive (rule learning: Benchenane et al., 2010; reward expectation and delivery: Hyman et al., 2011, 2017), metabolic (reward consumption: Horst and Laubach, 2013), and motivational (Jackson et al., 2006). These variables can all be challenging to control for, and, importantly for the present study, they all can vary significantly between days or during a task (Lee et al., 2006). Thus, we needed to use a task that was consistent from session to session regardless of how much experience the subject had with the task, how well the subject performed during the session (affecting the amount of reinforcement earned), or how much time had passed between sessions.

To isolate temporal effects, we strove to keep the memory information as simple as possible to minimize behavioral or cognitive factors. We used a naturalistic task (environment exposure) that is not reliant upon performance. Because the task features no overt goals or rewards (Figure 1), any potential influence from motivational differences, within session relearning, or working memory was minimized. Additionally, this task drives strong ACC and CA1 activity (Hyman et al., 2012) and theta interactions (Hyman et al., 2005). We hypothesized that if memory dependence transfers to the ACC, then during more remote recall, theta interactions should strengthen between the areas. Moreover, ACC theta activity should robustly affect CA1 during remote recall compared to initial encoding or recent recall.

RESULTS

Exploration Was Similar across All Sessions during the First Two Minutes

We first examined how gross locomotor activity changed over each environment exposure period to see if animals explored more during the initial few minutes of exposure. We normalized distance traveled values for each environment (Z transformed), before conducting a two-factor ANOVA (exposure minute [1–10] × retention interval [days since last exposure: 0, 1, 2, 7, or 14]). We found a significant main effect for exposure minute (F[9, 850] = 3.51, p = 2.82E-4) but no difference in retention interval (F[4, 850] = 0.02, p = 0.99) and no interaction effects (F[4, 850] = 1.01, p = 0.45) (Figure 2A). Post hoc tests illuminated that the amount of exploration changed minute to minute, but a similar pattern appeared on all days, in which distance traveled during the first 2–4 min was significantly greater than for the remaining time. This analysis revealed a behavioral window (first 120 s) with similar gross locomotor activity during both initial exposure and at all retention intervals. All subsequent behavioral

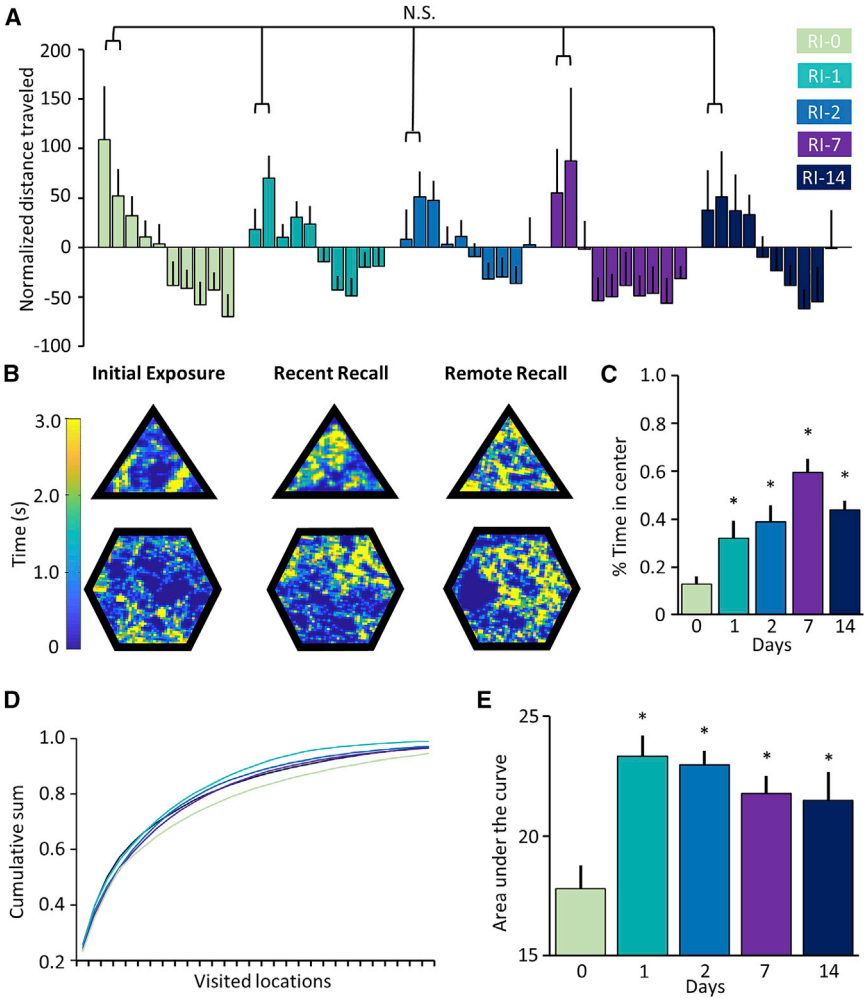

Figure 2. Behavioral Changes Occur When Subjects Are Re-exposed to an Environment

(A) Total distance traveled by exposure minute. Normalized distance traveled is on the y axis and time (minutes) on the x axis. In initial exposures and all recall sessions animals explored more in the first few minutes. No significant differences in distance traveled were found during the first 2 min across the different exposures ($p > 0.05$).

(B) Representative exploratory activity during initial, recent, and remote recall sessions. Note that animals spent more time in the center of the environment on recent and remote days compared with initial exposures.

(C) Proportion of time spent in center increases after initial exposure. Mean proportion of time spent in the center of each environment is on the y axis and retention interval is on the x axis.

(D) Cumulative sum and area under the curve for exploratory behavior. Mean cumulative sum values from all subjects and environments for each retention interval.

(E) Mean area under the curve of time spent in different locations throughout an environment. Note that significant increases appeared for all re-exposures compared with initial exposures. Thus, familiarity was apparent upon the second exposure but did not differ between recent and remote recall.

*$p < 0.05$.

and electrophysiological analyses were restricted to only the first 120 s of exposure, because this period allowed us to make comparisons with similar levels of gross locomotor activity.

Behavioral Changes Materialized after Initial Environment Exposure

To quantify habituation effects, we analyzed how much time subjects spent in the center of the environment compared with the periphery. During the initial exposure, subjects spent more time along the periphery; then, after habituating to an environment, animals spent more time in the center (see the example sessions in Figure 2B). We found a significant main effect in center-periphery ratios for days since last exposure ($F[4, 93] = 15.53$, $p = 1.12E\text{-}9$). Importantly, post hoc tests showed the center-periphery ratios changed following the first re-exposure, as all re-exposures (days 1, 2, 7, and 14) were significantly different from day 0 but not different from one another (see Figure 2C). Thus, it did not matter whether the re-exposure occurred 1 or 14 days after the last exposure ($p > 0.05$), which showed comparable memory recall at all retention intervals.

We also sought to measure habituation effects by investigating how much time animals spent in different locations within environments. If an animal explored a great deal, then it would have spent a similar amount of time in each location, but habituated animals should feel less of a need to explore the entire environment, and most of their time should be spent in just a few locations. Unlike the center-periphery analysis, where in the environment was immaterial, rather how many locations and for how long they were visited mattered. We first divided each environment into equal sized spatial bins and then examined the amount of time animals occupied each location (during the first 120 s). We compared the area under the curve (AUC) and found a significant main effect for days since last exposure ($F[4, 93] = 6.972$, $p = 6.26E\text{-}5$; Figures 2D and 2E). Post hoc tests reported significantly larger values for all days other than day 0 and that these retention days were not significantly different from one another ($p < 0.05$).

It was possible that the animals were merely habituating to open-field exposure, and as the number of exposures increased anxiety from being in the open field decreased. To control for this potential confound, we introduced a novel environment (environment G) during session 6 (see Figure 1A). Thus, on this day animals were first re-exposed to two environments after a 14 day retention interval (B and D), and then they were placed into a brand new environment (G). We hypothesized that if animals were exploring less and spending more time in the center on remote recall days because of decreased anxiety, then we should see similar behavioral patterns even in this novel

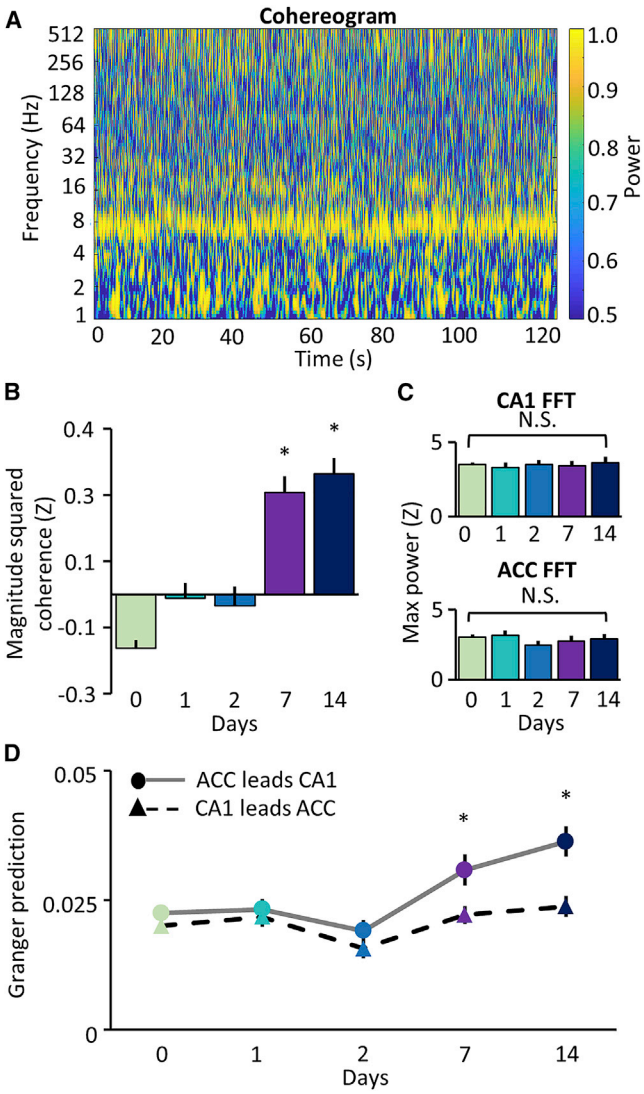

Figure 3. Increases in Theta Oscillatory Interactions during Remote Recall

(A) Example coherogram from the first 2 min of a remote recall exposure. Note high-powered coherence in the theta range (7–12 Hz).

(B) Normalized coherence between ACC and CA1 by retention interval. Significant changes in theta band coherence only appear during remote recall.

(C) No differences in normalized theta power in CA1 (top) and ACC (bottom).

(D) ACC leads CA1 theta during remote recall. Mean theta Granger prediction values are on the y axis, and retention interval in days is on the x axis. There were no differences in ACC lead and CA1 lead models for initial exposure and recent recall, but during both remote recall intervals, the ACC lead models had larger Granger predictive strength.

*$p < 0.0001$.

environment. We compared distance traveled and proportion of time spent in the center versus the periphery between session 6 environments D (RI-14) and G (RI-0) and the initial exposure to environment D (RI-0) during session 2. We found that environment G behavioral patterns were similar to the initial exposure to environment D and significantly different from the remote recall re-exposure to environment D (distance traveled, $F[2, 160] = 0.0012$, $p > 0.05$; center-periphery ratio, $F[2, 16] = 0.547$, $p = 0.015$; locations visited AUC, $F[2, 84] = 9.95$, $p = 0.0001$; see Figures S1A–S1C). These analyses suggest that changes in open-field behavior were due to memories of specific contexts and not anxiety or motivationally related processes linked to experience with the task itself. Furthermore, for all our main behavioral analyses, data were grouped by retention interval and sessions; thus the RI-0 group contained data from exposures ranging over 3 consecutive days. If merely being exposed to multiple environments was having an anxiety-decreasing effect, then our RI-0 values should have reflected this because these data mixed so many temporally separated exposures.

Together, our behavioral measures identified evidence of initial learning (i.e., habituation) and consistent recall over different retention intervals. These results demonstrated that the environment exposure task was ideal for finding any potential electrophysiological markers related to memory consolidation, because habituating to an environment was so simple that it occurred in one exposure and performance was similar on subsequent days. Critically, comparable contextual recall is dependent upon both HC (Wiltgen et al., 2010) and ACC function (Teixeira et al., 2006).

ACC-CA1 Coherence Increased during Remote Recall

Oscillatory coherence is thought to be a general indicator of communication between brain areas (Fries, 2005). Theta coherence between the HC and medial frontal cortex varies with working memory performance (Hallock et al., 2016), rule changes (Benchenane et al., 2010), and the type of information being processed (Place et al., 2016). Here, we tested whether such effects were also influenced by remote memory recall. A single-factor ANOVA (days since last exposure: 0, 1, 2, 7, or 14) found significant differences in coherence values ($F[4, 2,779] = 35.521$, $p = 2.011E-30$; Figures 3A and 3B). Post hoc tests showed that coherence was significantly higher on days 7 and 14 compared with initial exposure and recent recall ($p < 0.05$, Tukey's honestly significant difference [HSD] test). Importantly, no significant differences were found between initial exposures (day 0) and 1 or 2 day retention intervals ($p = 0.46$), demonstrating that the learning captured by our behavioral measures did not alter ACC-CA1 theta coherence. These two comparisons allowed us to isolate out familiarity-related (day 0 versus days 1 and 2) from retention interval-related changes (days 1 and 2 versus days 7 and 14). Thus, theta coherence was affected by the amount of time that had passed since the last exposure and not familiarity with an environment.

Although the above analyses showed that theta coherence values increased for longer retention intervals, it was possible that this was due merely to coincidental changes in ACC and CA1 theta oscillations. To control for this, we examined maximum power in the theta band (7–12 Hz), and there were no differences over retention intervals for both areas (CA1: $F[4, 172] = 0.345$, $p = 0.967$; ACC: $F[4, 172] = 0.802$, $p = 0.526$; Figure 3C).

Additionally, we found similar coherence values when animals were initially exposed to a novel environment during session 6 and during session 2, even though these sessions were separated by more than 2 weeks. Coherence for both initial exposures

was lower than remote recall exposures (F[2, 605] = 6.9317, p = 0.0011; Figure S1D). Thus, even though ACC-CA1 coherence was elevated during session 6 remote recall re-exposures, it returned to lower initial exposure and recent recall levels once animals entered a novel environment. These findings make it unlikely that any undetected anxiety-related effects were influencing ACC and CA1 electrophysiological activity. Together, these results clearly show the change in coherence values were altered by the consolidation process as opposed to other factors.

ACC Led CA1 during Remote Recall

Theta band coherence has been associated with ACC-CA1 interactions, and it is widely believed that such coherence is a prerequisite for successful communication (Gray, 1994), but this does not indicate which direction communications were flowing (i.e., CA1 to ACC or vice versa). To understand the direction of the neural interactions detected in our coherence analysis, we calculated Granger prediction values. Briefly, for this analysis univariate autoregressive models are created at various time steps for each signal. Then, bivariate models are created to see if the signal detected on one lead (X) is predictive of the signal recorded on the other lead (Y). We then compared the relative strength, or the difference in error from the univariate model, of bivariate models created in both directions.

Because our coherence analysis revealed increases in the theta band (Figure 3A), we compared mean Granger prediction values in this frequency range. A two-way ANOVA (direction × retention interval) revealed significant main effects (direction: F[1, 5,558] = 17.703, p = 2.6E-5; retention interval: F[4, 5,558] = 9.605, p = 9.73E-8) and a significant direction-by-retention interval interaction (F[4, 5558] = 2.858, p = 0.02). As can be seen in Figure 3D, Granger values indicated similar predictive strength in both directions (ACC leads or HC leads) during initial exposure and recent recall (p > 0.05). During remote recall exposures, ACC lead values were significantly larger than HC lead values (p < 0.0001) and increased from initial and recent ACC lead values (p < 0.0001). These results showed that ACC theta activity was predictive of HC theta during remote recall, indicating increased directional connectivity between the areas.

CA1 Gamma Was Modulated by ACC Theta during Remote Recall

The above results showed that increased ACC-CA1 theta interactions during remote recall were driven by the ACC, though how or if ACC theta was affecting hippocampal ensemble activity was still not known. We used multiple analyses to investigate these effects. First, we examined the amount of cross-frequency phase-amplitude coupling between theta activity in one area and gamma oscillations in the other. Such cross-frequency coupling is thought to differentiate between the effects of long range (theta) and local (gamma) communication (Sirota et al., 2008). We hypothesized that if a memory were consolidated to the ACC, recall should originate in the ACC. Like a spark that starts a fire, ACC output should initiate activity across neural ensembles in multiple brain areas. Thus, CA1 gamma activity should relate more strongly to ACC theta phase during long retention intervals (Figure 4A). We compared each possible ipsilateral pair of ACC (theta) and CA1 (gamma) recording leads for the first 120 s of each environment exposure. Overall, modulation index values were significantly affected by retention interval (F[4, 2779] = 10.652, p = 1.447E-08; Figure 4B). The significant differences emerged on day 7 and remained on day 14 (p < 0.001, Tukey's HSD test). No familiarity-related differences were found (day 0 versus day 1), but retention interval-related increases were apparent between days 1 and 7 or 14 (p < 0.0001) and days 2 and 7 or 14 (p < 0.05). Thus, as more time passed since the last visit, hippocampal gamma activity was more strongly modulated by ACC theta oscillations, implying that theta frequency ACC input drove hippocampal unit activity.

To control for whether this effect was unique to ACC theta, we also examined internal CA1 theta gamma phase-amplitude coupling and found no significant differences over the different retention intervals (F[4, 2779] = 2.772, p = 0.026E-4; Figure 4B). This indicates that indeed CA1 gamma was affected by ACC theta and that our above findings were not the by-product of changes in internal CA1 oscillatory coupling.

We also analyzed cross-frequency coupling in the opposite direction (CA1 theta phase to ACC gamma power), and the only significant difference was a decrease in coupling between recall day 0 and day 14 (F[4, 2779] = 5.2751, p = 3.126E-4; Figure 4C). This could possibly indicate that as ACC theta influence on CA1 increased, there was a corresponding decrease in CA1 influence on ACC gamma over time. As a control we also compared internal ACC theta gamma phase-amplitude coupling and found a weakly significant result overall (F[4, 2779] = 4.6835, p = 0.009; Figure 4C), but follow-up tests only revealed significant differences between initial exposure and 14 day retention intervals (p = 0.001, Tukey's HSD test). Remote recall was decreased from initial exposure, but no differences appeared between recent and remote recall, making it difficult to properly gauge this effect. Together these analyses show that the ACC-driven increased theta interactions detected on long retention intervals were significantly modulating local CA1 networks, and no comparable effects were found in the other direction.

More CA1 Units Were Phase Locked to ACC Theta during Remote Recall

In 34 recording sessions over seven animals we recorded 787 ACC cells and 612 CA1 cells that had at least 50 spikes during the first 120 s of each environment exposure period analyzed. The cells were separated by retention interval (see Figure 1A), yielding cell counts as follows: RI-0, 148 ACC and 94 CA1; RI-1, 139 ACC and 117 CA1; RI-2, 144 ACC and 167 CA1; RI-7, 132 ACC and 96 CA1; and RI-14, 224 ACC and 138 CA1.

We examined both CA1 theta oscillations' influence on ACC unit firing and ACC theta oscillations' influence on CA1 unit firing. We hypothesized that if memory information were consolidated to the ACC, readout of this memory should be driven by the ACC. This should manifest as both changes in how widespread and how strongly CA1 cells were affected by ACC theta rhythms. Conversely, if remote recall interactions were like those observed during working memory, then ACC units should be strongly affected by CA1 theta.

When we compared ACC unit phase locking to CA1 theta oscillations during the first 120 s of exposures, we found no significant

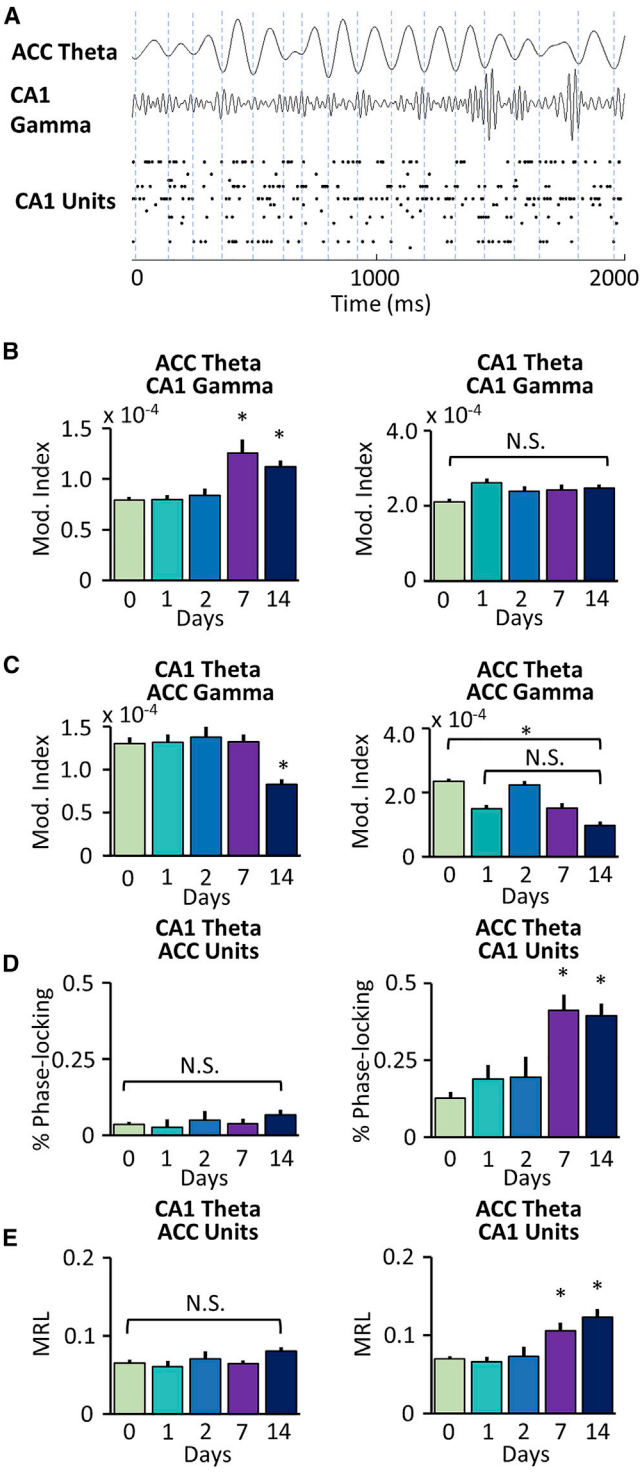

Figure 4. CA1 Gamma Power and Unit Spiking Are Modulated by ACC Theta during Remote Recall

(A) Representative remote recall trace showing theta-filtered ACC LFP, gamma-filtered CA1 LFP, and CA1 unit spiking.

(B) CA1 gamma power is modulated by ACC theta phase during remote recall. For both plots, modulation index is on the y axis and retention interval on the x axis. Left: ACC theta phase to CA1 gamma power cross-frequency coupling. Values increased for remote recall, showing the strong influence of ACC theta on CA1 circuits. Right: CA1 theta phase modulation of CA1 gamma does not change between different retention intervals.

(C) Theta modulation of ACC gamma does not increase during remote recall. For both plots, modulation index is on the y axis and retention interval on the x axis. Left: there is a decrease in CA1 theta phase to ACC gamma power coupling, but only on day 14. Right: ACC theta phase modulation of ACC gamma does not change between recent and remote recall.

(D) More CA1 units are phase locked to ACC theta during remote recall. In both plots, percentage of units significantly phase locked to theta rhythm in the other area is on the y axis, and retention interval is on the x axis. Left: the number of ACC units entrained to CA1 theta did not differ over days. Right: significantly more CA1 units were entrained to ACC theta on remote recall days.

(E) Average CA1 unit MRL values increased during remote recall. In both plots, MRL values are on y axis, and retention interval is on the x axis. Left: MRL values for ACC cells for CA1 theta; right: MRL values of CA1 cells for ACC theta.

*$p < 0.0001$.

differences by retention interval for both percentage of phase-locked units (multiple comparison-corrected Rayleigh's test of uniformity, $p < 0.000625$; $F[4, 782] = 0.898$, $p > 0.05$; Figure 4D) and average mean resultant length (MRL) ($F[4, 782] = 2.07$, $p > 0.05$; Figure 4E). The effects of CA1 theta oscillations on ACC unit activity do not change over time or as a factor of familiarity, indicating that network dynamics are different than during working memory. Concurrently, there were significant increases in the both the percentage of CA1 cells significantly phase locked to ACC theta oscillations ($F[4, 619] = 14.655$, $p = 1.91E-11$; Figure 4D) and mean MRL ($F[4, 619] = 12.40$, $p = 1.04E-9$; Figure 4E). The increases over initial exposure (i.e., day 0) first appeared on retention day 7 and remained elevated at day 14 ($p < 0.001$, Tukey's HSD test). Notably, there were no changes for either percentage of cells phase locked or MRL values between initial exposure and recent recall days, indicating that familiarity did not affect CA1 unit phase locking to ACC theta. Rather, the strong increase between recent (days 1 and 2) and remote recall (days 7 and 14) ($p < 0.001$ for all) signaled that time since last exposure was the operative variable. Thus, CA1 unit entrainment to ACC theta rhythms changed in a similar pattern over time as coherence, Granger prediction, and theta-gamma phase coupling.

CA1 and ACC Environmental Context Ensemble States Grew More Distinct

We previously showed that ACC ensemble activity states were more distinct for two different environmental contexts than CA1 ensembles (Hyman et al., 2012). The present study used the same task but introduced a memory component by adding more environmental contexts and then re-exposing subjects to each environment at different retention intervals. It was previously reported that larger amounts of cFos and α-CaMKII were found in ACC following remote recall (Bontempi et al., 1999; Frankland et al., 2001), suggesting stronger ACC activity during these re-exposures. Higher firing rates or more distinct changes in individual unit environmental responses would likely manifest as increased separation in multiple single-unit activity (MSUA) state space (Hyman et al., 2012; Ma et al., 2016). Essentially, this analysis examines the heterogeneity between multidimensional samples. The more distinct the samples, the more

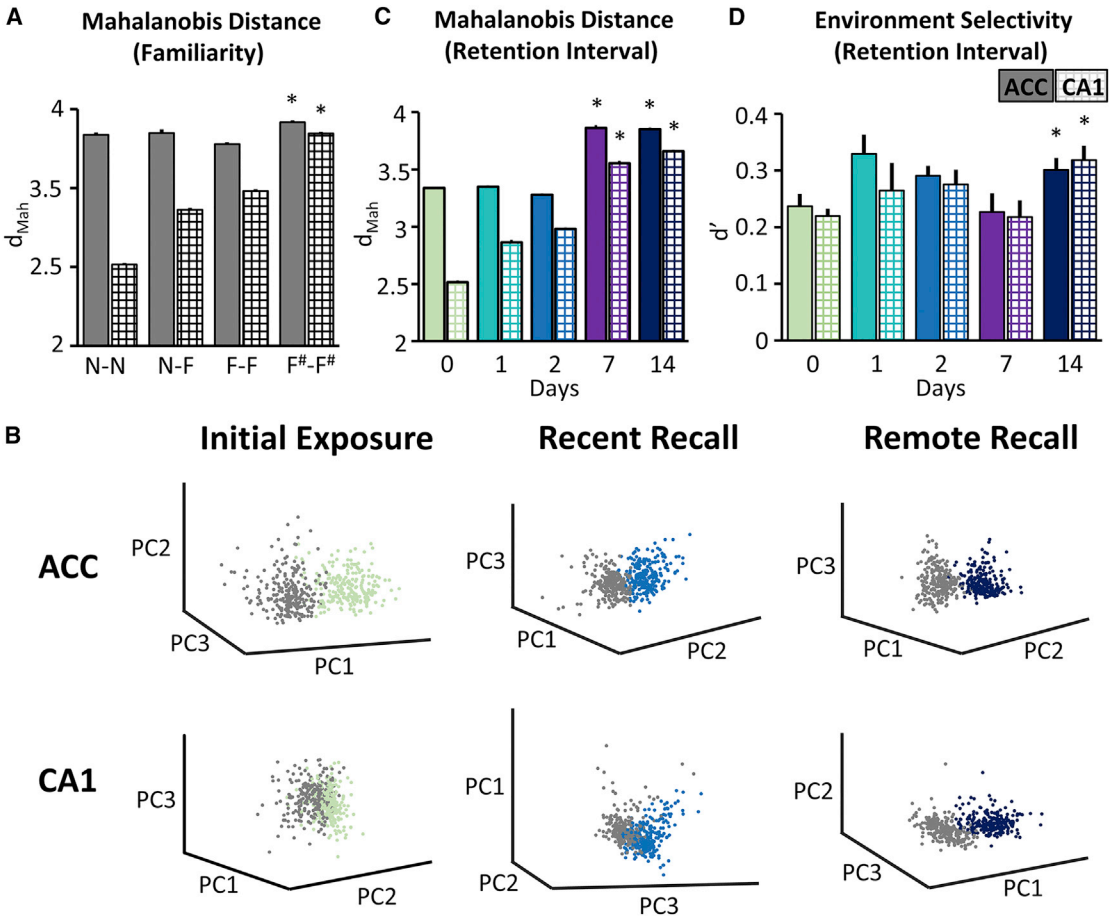

Figure 5. Environmental Context Information Increases during Remote Recall in Both ACC and CA1

(A) Novelty and familiarity differentially affect ACC and CA1. Mahalanobis distance (dMah) values are on the y axis, and type of comparison is on the x axis. Ensemble activity state environmental separation was greater in ACC for comparisons that involved novelty or remote recall. CA1 ensembles more distinctly represented recent and remotely recalled familiar environments than novel. NN, novel to novel; NF, novel to familiar; FF, familiar to familiar. #Including remote recall sessions.

(B) MSUA spaces from representative ensembles for different exposure types. In all plots, each dot represents the activity state of the ensemble during 500 ms. Gray dots show times from the first environment, and the colored dots show the next. Plots are shown in PC space, but all analyses were performed in the full high-dimensional space. Notice how the CA1 remote recall MSUA space (far right) shows clear clustering and separation on the basis of environment similar to the ACC spaces.

(C) Ensemble environmental context states are more distinct during remote recall. dMah is on the y axis, and retention interval in days since last exposure is on the x axis. Separation in both areas was increased during remote recall, with the biggest changes seen in the CA1.

(D) Individual cell environmental selectivity increased at the longest retention intervals. d′ values are on the y axis, and days since last exposure is on the x axis. On average, unit activity in both areas had more information distinguishing one environment over another during 14 day recall compared with initial exposure.

In all plots, ACC values are shown in solid bars and CA1 are in checkerboard. *p < 0.0001.

divergent the network states and in turn the greater the amount of information each state relays about an individual environment. In the current experiment, we hypothesized that the environmental context representations should become more distinct from each other during remote recall.

We first sought to isolate familiarity from retention interval length, so we restricted this analysis to the first three sessions (including days 0, 1, and 2; see Figure 1A). For all comparisons, we calculated Mahalanobis distance (dMah) in the full high-dimensional space, and all comparisons were made between time points corresponding to the first 120 s in one environment compared with the first 120 s in the next environment. A two-way ANOVA (recording area [CA1, ACC] × familiarity category [novel to novel, novel to familiar, familiar to familiar]) found significant main effects for both recording area (F[1, 11,994] = 860.4298, p < 1E-100) and familiarity (F[2, 11994] = 81.797.534, p = 4.2E-91). ACC ensembles had significantly greater dMah values than CA1 ensembles for all comparisons (p < 0.0001; see Figure 5A), replicating our previous finding (Hyman et al., 2012). Interestingly, comparisons between CA1 ensembles found more separation when at least one familiar environment was included, but no similar effect was found in ACC. In the ACC, the largest differences in ensemble states were found in novel-to-novel comparisons, while in CA1 familiar-to-familiar comparisons were the largest. Together a picture emerges of ACC ensembles as more reactive to novelty and CA1 ensembles

to familiarity (at least during recent recall), which is consistent with previous results (Wilson and McNaughton, 1993; Weible et al., 2012). This might suggest that CA1 learns faster than the ACC, but further experimentation is required. Overall, this analysis detected changes in environmental context information in both areas that correlated with the different behavioral patterns we found in novel and familiar environments.

We next explored how the passage of time, and thus memory consolidation, affected environmental context information by incorporating the two long retention sessions (5 and 6; see Figure 1A). We first repeated the previous analysis, but this time included familiar-to-familiar comparisons from day 7 and 14, along with the novel-to-familiar comparison on day 14. Again, we found significant main effects for both recording area (F[1, 17,994] = 1111.50, p < 1E-100; Figure 5A) and familiarity (F[2, 17,994] = 653.49, p < 1E-100) in dMah values. Follow-up tests showed the familiar-to-familiar distances were now larger in the ACC and CA1 compared to when only the recent recall sessions were included (p < 0.0001).

We next wanted to isolate retention interval from familiarity. To test this directly we needed to regroup the same dMah values from above, because the uneven distribution of familiarity categories over days made a single ANOVA with both retention interval and familiarity not possible. We formed groups on the basis of the retention interval for the first environmental context in each dMah comparison (i.e., environment A in an AB comparison). This left us with the same five retention intervals analyzed previously (days 0, 1, 2, 7, and 14). Both areas showed increases in environmental context clustering on remote recall days, and this can be seen most strikingly in CA1 ensembles (Figure 5B). Notice how during remote recall (far right) the different colored dots are more tightly grouped together into clusters, and those clusters are more separated. A two-way ANOVA (recording area × retention interval) found both main effects (area: F[1, 17,990] = 1,736.9, p < 1E-100; interval: F[4, 17,990] = 1,165.6, p < 1E-100) and a significant interaction (F[4, 17,990] = 140.67, p < 1E-100) (Figure 5C). Follow-up tests showed significantly increased dMah values between areas at each retention interval (p < 0.0001). In fact, during remote recall, CA1 ensembles had such well-separated clusters that they resembled ACC ensembles, which would be expected with an increase in information flowing from the ACC to CA1.

At a single-cell level, the picture was slightly different when we calculated the selectivity indices for all cells comparing the same two 120 s windows analyzed above. We found no significant effect of recording area (F[1, 1,399] = 0.0825, p = 0.774), but we did find an effect for retention interval (F[4, 1,399] = 3.3926, p = 0.009) (Figure 5D). However, no significant area-by-interval interaction was found (F[4, 1,399] = 1.537, p = 0.1888), indicating that the cells in both areas had similar degrees of preference for one environmental context over another and that cells in both areas formed stronger preferences over time.

CA1 Context Information Was Related to ACC Theta Phase Locking

Last, we examined theta entrainment to relate together interarea theta interactions and ensemble environmental context encoding. We hypothesized that if environmental context information were flowing from the ACC to CA1, then CA1 ensembles with larger percentages of ACC theta phase-locked units and higher mean MRL values would also have higher dMah values. Alternatively, increases in theta coherence during remote recall could be indicative of overall increased communication back and forth, and if so, we would expect dMah and interarea theta entrainment to be related in both directions.

We fit linear models using dMah values (from that ensemble) as the predictors and theta entrainment as the observed values. We found significant linear fits for both ACC theta entrainment measures (mean MRL values: R^2 = 0.298, t(8,998) = 61.876, p < 1E-100; percentage phase locked: R^2 = 303, t(8,998) = 62.548, p < 1E-100), indicating that CA1 ensemble dMah values and ACC theta entrainment were strongly positive correlated (Figures 6A and 6B). Thus, the more theta entrained a given CA1 ensemble, the stronger the MSUA state space environmental context representation. However, when we compared interactions in the other direction we found that ACC ensemble dMah values were only weakly related to CA1 theta (MRL: R^2 = 0.00006, t(8,998) = −2.361, p = 0.018; percentage phase locked: R^2 = 0.0072, t(8,998) = −8.0537, p = 9.056E-16). As can be seen in Figures 6C and 6D, ACC ensemble dMah values negatively correlate with both measures of CA1 theta entrainment, suggesting that CA1 theta input decreases ACC environmental context representation distinctiveness. These results suggest that ACC ensemble environmental context representations were not altered by CA1 theta entrainment, but CA1 ensemble information content was strongly affected by ACC theta. Altogether, these results imply that environmental context information was transferred from ACC to CA1.

Because both dMah and theta entrainment increased on remote recall exposures, it was difficult to determine whether both were changing at the same time or one variable was driving the other. Rather, the global variance (changes over days) was so large that it was difficult to assess the how theta entrainment affected dMah on a case-by-case basis (i.e., local variance). To disentangle these variables, we took two different approaches. First, we separately fit linear models to both CA1 dMah and theta entrainment (MRL) using retention interval (day 0 = 1, day 1 = 2, day 2 = 3, day 7 = 4, day 14 = 5) as the predictors and found significant fits for both variables (p < 1E-100). We then compared the residual values, allowing us to examine local variance and determine whether these two factors covaried from linear fits. More specifically, when one ensemble's dMah drifted from the linear fit, did its theta entrainment also differ and in the same direction? To test this, we fit a linear model to the residual values and found a good fit for mean MRL and dMah values (R^2 = 0.117, t(8,998) = 334.52, p < 1E-100; Figure 6E).

Our second approach examined single-cell environmental context information coding and interarea theta phase locking. Above, we found that both ACC and CA1 single neurons were more selective for one environment over another during remote recall. We now wanted to assess the role of external theta entrainment on these effects. Using the d-prime environmental selectivity indices calculated before, we grouped on the basis of three factors: area (CA1 or ACC), retention interval (0, 1, 2, 7, or

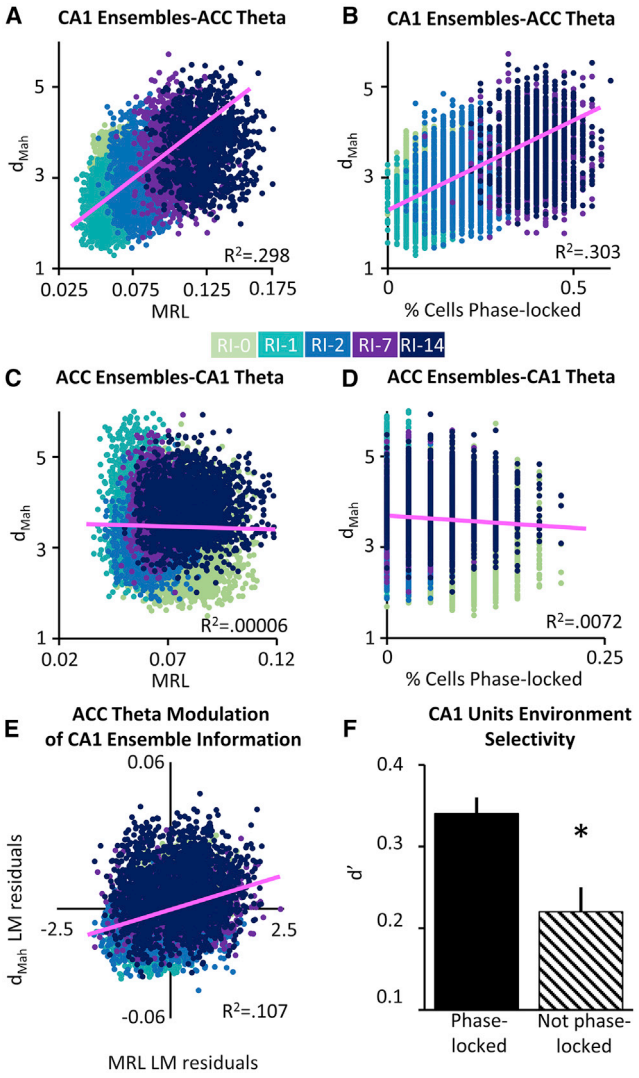

Figure 6. Environmental Information in CA1 Ensembles Is Related to Degree of ACC Theta Entrainment

(A) Larger CA1 ensemble environmental separation correlates with larger average ACC theta entrainment. dMah values are on the y axis and ensemble mean MRL on the x axis. Dot color indicates retention interval.

(B) Higher proportion of CA1 cells entrained to ACC theta correlated with ensemble environmental context separation. dMah values are on the y axis, and percentage of ACC theta entrained cells are on the x axis.

(C and D) ACC ensemble environmental states are not affected by CA1 theta rhythms. Although the strength (mean MRL) (C) and spread (percentage phase locked) (D) of CA1 theta modulation of ACC units decreased and ACC dMah values increased, these two factors were only weakly correlated.

(E) Theta modulation affected within recall day variance of CA1 ensemble environmental activity states. The y axis shows residual values from fitting a linear model to CA1 ensemble dMah values, and the x axis shows the residuals from a separate linear model of mean MRL values from the same ensembles. This analysis controlled for changes in these values over days and showed that even within days, the more ACC theta entrained an ensemble of CA1 cells, the greater the amount of environmental context information.

(F) CA1 unit environmental preference is stronger in ACC theta entrained cells. Selectivity index (d′) values are on the y axis. ACC theta phase-locked neurons carried more information about which environmental context the subject was currently in.

14 days), and whether the cell was significantly phase locked to ACC theta rhythm. The three-way ANOVA returned null results, except for one comparison: ACC theta entrainment. Once this factor was included, the apparent retention interval effect reported above (Figure 5D) disappears (F[4, 1,398] = 1.792, p = 0.1280). Thus, the only factor influencing CA1 environmental selectivity was whether that cell was ACC theta entrained or not (F[1, 1,398] = 5.9244, p = 0.0151; Figure 6F). With these results we can conclude that ACC theta entrainment profoundly affected both CA1 single-unit and ensemble environmental information content. Simply, how strongly a CA1 ensemble entrained to ACC theta rhythms predicted how distinctly that same ensemble represented two environmental contexts, suggesting that the important factor differentiating recent and remote recall was the proliferation of ACC theta modulation. Over the consolidation process, these effects grew more widespread, which led to CA1 ensembles with significantly better environmental context information.

DISCUSSION

Interactions between the ACC and CA1 strongly increased as memories progressed from recent to more remote. Multiple different electrophysiological markers (theta frequency Granger prediction, theta-gamma phase-amplitude coupling, interarea theta entrainment) pointed to ACC theta modulation of CA1 as the main driving force behind this effect. Concurrently, the amount of environmental context information in CA1 and ACC unit spike trains and ensembles also increased. These measures were related, such that more ACC theta entrainment amounted to greater CA1 cell context information. Over time, ACC theta entrainment of CA1 cells spread, and thus environmental context information was increased over the whole CA1 population. Together, these results are consistent with the transference of environmental context memory dependence to the ACC during consolidation and show that during remote memory recall information is passed from the ACC to CA1 via theta rhythm interactions.

A Possible Thalamic Route for ACC Theta Modulatory Control of HC

There are multiple possible mechanistic avenues through which ACC theta could modulate CA1 activity, including both direct and indirect projections. Most work on theta interactions between the ACC and HC has concentrated on the dense reciprocal connections that pass through the reuniens nucleus of thalamus (RE; Carr and Sesack, 1996; Hoover and Vertes, 2007). These pathways contain bidirectional excitatory connections (Vertes, 2002; Di Prisco and Vertes, 2006; Vertes, 2006), as well as excitatory collateral projections that extend to both HC and ACC (Hoover and Vertes, 2012). This makes the RE-based cortico-thalamo-hippocampal circuit a likely path via which ACC theta could modulate the HC. Indeed, RE field potentials are coherent with both HC and medial frontal theta oscillations (Roy et al., 2017), and RE neurons are phase locked with hippocampal theta (Ito et al., 2018). Reports have found that working memory ACC-HC theta interactions decrease when RE is disrupted and behavioral performance is also impaired (Hallock et al.,

2016; Ito et al., 2015, 2018). Interestingly, such spatial working memory tasks are dependent upon both the HC and ACC (Floresco et al., 1997; Izaki et al., 2000; Lee and Kesner, 2003; Churchwell et al., 2010), suggesting that RE-based interactions are integral to proper working memory function. Additionally, RE inactivation also impairs behavioral flexibility leading to perseveration in win-shift tasks (Viena et al., 2018) and an inability to generalize response strategies between contexts (Linley et al., 2016), which indicates a broader role in cognition for RE-based interactions. Although the current study involved a completely different task, it is conceivable that these same connections could mediate interactions in the opposite direction during remote recall. Indeed, two notable reports have shown medial frontal theta affected hippocampal processing (Onslow et al., 2011; Place et al., 2016), though neither of these experiments delved into possible mechanisms. Thus, it is possible that during remote recall, ACC efferents stimulate RE neurons, which in turn modulate CA1 units and field potentials.

Eichenbaum (2017a) suggested that the medial frontal cortex could exert top-down control over the HC via bidirectional perirhinal and/or entorhinal cortical connections (Burwell and Amaral, 1998; Witter et al., 2000; Apergis-Schoute et al., 2006), and it is conceivable that the present results are indeed the manifestation of top-down control. These connections are more difficult to isolate than those passing through the RE nucleus and have not been studied intensively, but hopefully, future studies will help reveal what role they have in medial frontal-HC interactions. Additionally, both the HC and ACC also have common theta-related connections with other areas, such as the raphe nucleus (Vertes and Kocsis, 1994; Chandler et al., 2013), reticular formation (McNaughton and Sedgwick, 1978; Sesack et al., 1989), VTA (Fujisawa and Buzsáki, 2011), and septum (Varela et al., 2014). It is possible these non-thalamic routes are mediating remote recall network dynamics, though these connections have not been thoroughly evaluated for any potential role in ACC-HC interactions. Another possibility are the direct connections from ACC to dorsal CA1 reported by Rajasethupathy et al. (2015), however, the sparsity of such ACC to CA1 projecting neurons demands a cautious approach when hypothesizing their function. With that said, these direct connections are a tantalizing possible source by which ACC theta input could modulate CA1 activity, however, the most likely explanation is that such effects arise through multisynaptic interactions through the mediodorsal thalamus.

ACC-Driven Memory Retrieval

Bontempi et al. (1999) were the first to reveal a link between medial frontal areas and recall of remote environmental context information. Since then, more detailed anatomical studies shown that these effects occur in both dorsal and ventral areas along the medial wall of the frontal cortex (Wang and Cai, 2008). Similar effects have been documented for both appetitive and aversive conditioning tasks (Restivo et al., 2009; Frankland and Bontempi, 2005), suggesting that a more general form of memory (i.e., context) is consolidated to medial frontal cortex. Correspondingly, Kitamura et al. (2017) found that the network of medial frontal cells that became active during contextual fear learning could not be reactivated by cue presentation until 2 weeks after initial learning. Even though the same cells were part of this network, some maturation of the ensemble took place over the intervening period that made the network sensitive to recall cues. Perhaps the increase we observed in ACC ensemble representations over time is indicative of this idea. Although the Kitamura et al. (2017) study strongly suggests the storage of a contextual memory, our work provides some evidence of how this engram activation may affect the whole memory retrieval network. Indeed, it has been proposed that during remote recall the medial frontal cortex plays a role tantamount to the HC in recent recall. Thus, it coordinates reactivation of a memory trace across a broad neural network involving multiple brain areas (Maviel et al., 2004; Frankland and Bontempi, 2005; Blum et al., 2006; Eichenbaum, 2017b).

It should be noted that the task we used did not rely on emotional responses, and it is possible that the networks described here could react differently when emotional arousal is high. In fact, both the ACC (Shidara et al., 2005; Steenland et al., 2012) and HC (Sinnamon and Schwartzbaum, 1973) are strongly activated by emotional arousal, but similar contextual recall deficits are observed following ACC perturbation for both positive and negative emotional states (Maviel et al., 2004; Restivo et al., 2009). Additionally, ACC and HC networks notoriously respond to seemingly every possible event, as if they are providing a record of ongoing experience (Duncan and Owen, 2000; Eichenbaum, 2004). Thus, it is reasonable to conclude that the present results should extend to all tasks regardless of motivational valence, but certainly, this needs further experimentation to determine.

ACC Effects on HC Function

Although studies in animal models suggest that different memory networks are engaged in encoding and remote recall (Quillfeldt et al., 1996; Takehara et al., 2003), this idea is based on changes in memory recall dependence from the HC for recent memories (Squire and Alvarez, 1995; Bayley et al., 2003; Frankland et al., 2006; Ding et al., 2008) to the medial frontal cortex for remote (Maviel et al., 2004; Blum et al., 2006). However, imaging and recording studies in humans report similar networks of structures are activated during both memory encoding or recent recall and retrieval (Piolino et al., 2004; Viard et al., 2007, 2010; Rugg and Vilberg, 2013; Conejo et al., 2013; Kragel et al., 2017). Concurrently, Conejo et al. (2013) found that metabolic activity linked with functional interactions between the medial frontal cortex and HC was consistent throughout the memory process. However, chemogenetic inactivation of ACC cells impaired only remote recall and not recent (Varela et al., 2016). To square these apparently contradictory findings, it has been suggested that the hippocampal subfields are differentially engaged during encoding and remote recall (Hasselmo et al., 2002). The dentate gyrus (DG) is thought to perform pattern separation (presumably important for encoding new memories), and the CA fields are involved in pattern completion (important for retrieval). Most of these results have been based on lesion and inactivation studies of the subfields, so it is not clear how this could play out in the intact system. Given the strength of HC perforant path connections (Del Ferraro et al., 2018), it is far from obvious how the input of the DG could be selectively minimized during remote memory

recall. This would be necessary so that the orthogonalized DG output does not control CA1 and, thus, hippocampal output via the subiculum. The present results suggest that ACC-driven theta modulation may be a mechanism for this operation. ACC theta modulation could be biasing CA1 units toward ACC inputs, which would effectively minimize perforant path input. In such a model, ACC signals would cut internal hippocampal processing off at the pass and in turn control hippocampal output. In this way, remotely recalled ACC traces could control retrieval across the entire memory network by using the medial temporal lobe's connections with the rest of the brain. This creates the possibility that area CA1 may be involved in ACC directed remote memory retrieval, while simultaneously, DG function remains the same as during encoding, a possibility that is ripe for future testing. Such dynamics would lead to comparable levels of activity across the HC during encoding and remote retrieval, as is seen in human imaging results, even though memory dependence has changed over the course of consolidation.

These results present a mechanism for how the contextual memory system solves the important computational problem of separating memory encoding from retrieval, supporting the ideas put forward by Eichenbaum (2017a). It is possible that during remote recall of other types of information, other areas influence CA1 unit activity via theta modulation and that this is a common mechanism. It is also possible that the ACC has a unique role in remote memory retrieval, perhaps due to the global nature of contextual information, and thus is acting like the HC for remote recall but does so by controlling CA1 activity as a backdoor way to control HC output.

Alternatively, it is also possible that the observed effects are independent of the ACC and are either mediated by another neural area or somehow the product of internal hippocampal processes. Unit spatial responses in the HC do stabilize over the course of days (Frank et al., 2004; Attardo et al., 2018), so it is possible that over longer periods the hippocampal code changes even more. Once stable, hippocampal responses are remarkably durable with consistent spatial mapping observed over days and months (Muller and Kubie, 1987; Thompson and Best, 1990; Kinsky et al., 2018), however, in each of these studies, animals were exposed to the familiar environments multiple times in the intervening periods. This could possibly make the memories labile again as they undergo reconsolidation (Dudai and Eisenberg, 2004; McKenzie and Eichenbaum, 2011). Furthermore, it is possible that individual CA1 cells maintain strong place cell-like firing, but other cells change their context specific activity over consolidation. If so, the present results are not inconsistent with these previous findings, because those studies concentrated on cells with place fields established during initial learning and stabilized during recent recall. Alternatively, it has been proposed that the HC reconstructs consolidated neocortical memories into spatially coherent assemblies (Barry and Maguire, 2018). This may explain the similarities between the remote CA1 and ACC context representations, because CA1 could be using the ACC representation as the contextual foundation of its reconstruction.

Additionally, it is possible that a third neural area could drive both the ACC and HC during remote recall. For example, the VTA entrains both areas during working memory (Fujisawa and Buzsáki, 2011) and could do the same during remote recall. However, it is worth mentioning that the ACC can also drive VTA activity during high-effort responses (Elston and Bilkey, 2017; Elston et al., 2019), and one could argue that remote recall is a high-effort cognitive process. All these possibilities require further experimentation to evaluate, but given the data presented here, the simplest explanation is that the ACC is driving CA1 activity via theta oscillations during remote recall.

Conclusions

The present findings show robust changes in ACC-CA1 network dynamics as time passes from the last experience. These findings are consistent with the transference of contextual memory dependence, or consolidation, from the HC to the ACC. Furthermore, theta rhythm interactions are a likely mechanism for remote memory retrieval, which manifests in two ways as memories mature: CA1 units are more strongly modulated by ACC theta oscillations, and CA1 ensembles possess information that is similar to ACC ensemble contextual representations.

STAR★METHODS

Detailed methods are provided in the online version of this paper and include the following:

- KEY RESOURCES TABLE
- CONTACT FOR REAGENT AND RESOURCE SHARING
- EXPERIMENTAL MODEL AND SUBJECT DETAILS
- METHOD DETAILS
  - Surgery and Electrophysiology
  - Behavior
  - Histology
- QUANTIFICATION AND STATISTICAL ANALYSIS
  - Behavioral Analysis
  - Analysis of Continuous Data
  - Coherence
  - Granger Prediction
  - Theta-Gamma Cross Frequency Phase-Amplitude Coupling
  - Analysis of Unit Data
  - Unit Theta Phase-Locking
  - Mahalanobis Distance
  - Selectivity Index
- DATA AND SOFTWARE AVAILABILITY

SUPPLEMENTAL INFORMATION

Supplemental Information can be found online at https://doi.org/10.1016/j.celrep.2019.04.080.

ACKNOWLEDGMENTS

This work was supported by a grant from the Office of Economic Development at the University of Nevada Las Vegas (UNLV). We would like to thank J. Kinney, C. Lapish, and J. Seamans for their comments on the manuscript and discussion of the project. We would like to thank L. Crew, R. Francis, A. Ortiz, K. Zha, and N. Kaplan for their help collecting the data. The publication fees for this article were supported by the UNLV University Libraries Open Article Fund.

AUTHOR CONTRIBUTIONS

R.A.W. and J.M.H. designed the experiment. R.A.W. collected the data. R.A.W. and J.M.H. analyzed the data and wrote the manuscript.

DECLARATION OF INTERESTS

The authors declare no competing interests.

Received: January 15, 2019
Revised: March 18, 2019
Accepted: April 17, 2019
Published: May 21, 2019

REFERENCES

Adcock, R.A., Thangavel, A., Whitfield-Gabrieli, S., Knutson, B., and Gabrieli, J.D. (2006). Reward-motivated learning: mesolimbic activation precedes memory formation. Neuron *50*, 507–517.

Alain, C., Woods, D.L., and Knight, R.T. (1998). A distributed cortical network for auditory sensory memory in humans. Brain Res. *812*, 23–37.

Amodio, D.M., and Frith, C.D. (2006). Meeting of minds: the medial frontal cortex and social cognition. Nat. Rev. Neurosci. *7*, 268–277.

Apergis-Schoute, J., Pinto, A., and Paré, D. (2006). Ultrastructural organization of medial prefrontal inputs to the rhinal cortices. Eur. J. Neurosci *24*, 135–144.

Attardo, A., Lu, J., Kawashima, T., Okuno, H., Fitzgerald, J.E., Bito, H., and Schnitzer, M.J. (2018). Long-term consolidation of ensemble neural plasticity patterns in hippocampal area CA1. Cell Rep. *25*, 640–650.e2.

Barnett, L., and Seth, A.K. (2014). The MVGC multivariate Granger causality toolbox: a new approach to Granger-causal inference. J. Neurosci. Methods *223*, 50–68.

Barry, D.N., and Maguire, E.A. (2018). Remote memory and the hippocampus: a constructive critique. Trends Cogn. Sci. *23*, 128–142.

Bayley, P.J., Hopkins, R.O., and Squire, L.R. (2003). Successful recollection of remote autobiographical memories by amnesic patients with medial temporal lobe lesions. Neuron *38*, 135–144.

Benchenane, K., Peyrache, A., Khamassi, M., Tierney, P.L., Gioanni, Y., Battaglia, F.P., and Wiener, S.I. (2010). Coherent theta oscillations and reorganization of spike timing in the hippocampal- prefrontal network upon learning. Neuron *66*, 921–936.

Blum, S., Hebert, A.E., and Dash, P.K. (2006). A role for the prefrontal cortex in recall of recent and remote memories. Neuroreport *17*, 341–344.

Bontempi, B., Laurent-Demir, C., Destrade, C., and Jaffard, R. (1999). Time-dependent reorganization of brain circuitry underlying long-term memory storage. Nature *400*, 671–675.

Burwell, R.D., and Amaral, D.G. (1998). Perirhinal and postrhinal cortices of the rat: interconnectivity and connections with the entorhinal cortex. J. Comp. Neurol *391*, 293–321.

Buzsáki, G. (1986). Hippocampal sharp waves: their origin and significance. Brain Res. *398*, 242–252.

Carr, D.B., and Sesack, S.R. (1996). Hippocampal afferents to the rat prefrontal cortex: synaptic targets and relation to dopamine terminals. J. Comp. Neurol. *369*, 1–15.

Chandler, D.J., Lamperski, C.S., and Waterhouse, B.D. (2013). Identification and distribution of projections from monoaminergic and cholinergic nuclei to functionally differentiated subregions of prefrontal cortex. Brain Res. *1522*, 38–58.

Churchwell, J.C., Morris, A.M., Musso, N.D., and Kesner, R.P. (2010). Prefrontal and hippocampal contributions to encoding and retrieval of spatial memory. Neurobiol. Learn. Mem. *93*, 415–421.

Conejo, N.M., Cimadevilla, J.M., González-Pardo, H., Méndez-Couz, M., and Arias, J.L. (2013). Hippocampal inactivation with TTX impairs long-term spatial memory retrieval and modifies brain metabolic activity. PLoS ONE *8*, e64749.

Del Ferraro, G., Moreno, A., Min, B., Morone, F., Pérez-Ramírez, Ú., Pérez-Cervera, L., Parra, L.C., Holodny, A., Canals, S., and Makse, H.A. (2018). Finding influential nodes for integration in brain networks using optimal percolation theory. Nat. Commun. *9*, 2274.

Delorme, A., and Makeig, S. (2004). EEGLAB: an open source toolbox for analysis of single-trial EEG dynamics including independent component analysis. J. Neurosci. Methods *134*, 9–21.

Devinsky, O., Morrell, M.J., and Vogt, B.A. (1995). Contributions of anterior cingulate cortex to behaviour. Brain *118*, 279–306.

Di Prisco, G.V., and Vertes, R.P. (2006). Excitatory actions of the ventral midline thalamus (rhomboid/reuniens) on the medial prefrontal cortex in the rat. Synapse *60*, 45–55.

Ding, H.K., Teixeira, C.M., and Frankland, P.W. (2008). Inactivation of the anterior cingulate cortex blocks expression of remote, but not recent, conditioned taste aversion memory. Learn. Mem. *15*, 290–293.

Dudai, Y. (2004). The neurobiology of consolidations, or, how stable is the engram? Annu. Rev. Psychol. *55*, 51–86.

Dudai, Y., and Eisenberg, M. (2004). Rites of passage of the engram: reconsolidation and the lingering consolidation hypothesis. Neuron *44*, 93–100.

Duncan, J., and Owen, A.M. (2000). Common regions of the human frontal lobe recruited by diverse cognitive demands. Trends Neurosci. *23*, 475–483.

Durstewitz, D., Vittoz, N.M., Floresco, S.B., and Seamans, J.K. (2010). Abrupt transitions between prefrontal neural ensemble states accompany behavioral transitions during rule learning. Neuron *66*, 438–448.

Eichenbaum, H. (2004). Hippocampus: cognitive processes and neural representations that underlie declarative memory. Neuron *44*, 109–120.

Eichenbaum, H. (2017a). Prefrontal-hippocampal interactions in episodic memory. Nat. Rev. Neurosci. *18*, 547–558.

Eichenbaum, H. (2017b). On the integration of space, time, and memory. Neuron *95*, 1007–1018.

Elston, T.W., and Bilkey, D.K. (2017). Anterior cingulate cortex modulation of the ventral tegmental area in an effort task. Cell Rep. *19*, 2220–2230.

Elston, T.W., Croy, E., and Bilkey, D.K. (2019). Communication between the anterior cingulate cortex and ventral tegmental area during a cost-benefit reversal task. Cell Rep. *26*, 2353–2361.e3.

Floresco, S.B., Seamans, J.K., and Phillips, A.G. (1997). Selective roles for hippocampal, prefrontal cortical, and ventral striatal circuits in radial-arm maze tasks with or without a delay. J. Neurosci. *17*, 1880–1890.

Frank, L.M., Stanley, G.B., and Brown, E.N. (2004). Hippocampal plasticity across multiple days of exposure to novel environments. J. Neurosci. *24*, 7681–7689.

Frankland, P.W., and Bontempi, B. (2005). The organization of recent and remote memories. Nat. Rev. Neurosci. *6*, 119–130.

Frankland, P.W., O'Brien, C., Ohno, M., Kirkwood, A., and Silva, A.J. (2001). α-CaMKII-dependent plasticity in the cortex is required for permanent memory. Nature *411*, 309–313.

Frankland, P.W., Bontempi, B., Talton, L.E., Kaczmarek, L., and Silva, A.J. (2004). The involvement of the anterior cingulate cortex in remote contextual fear memory. Science *304*, 881–883.

Frankland, P.W., Ding, H.K., Takahashi, E., Suzuki, A., Kida, S., and Silva, A.J. (2006). Stability of recent and remote contextual fear memory. Learn. Mem. *13*, 451–457.

Fries, P. (2005). A mechanism for cognitive dynamics: neuronal communication through neuronal coherence. Trends Cogn. Sci. *9*, 474–480.

Fujisawa, S., and Buzsáki, G. (2011). A 4 Hz oscillation adaptively synchronizes prefrontal, VTA, and hippocampal activities. Neuron *72*, 153–165.

Geweke, J. (1982). Measurement of linear dependence and feedback between multiple time series. J. Am. Stat. Assoc. *77*, 304–313.

Gray, C.M. (1994). Synchronous oscillations in neuronal systems: mechanisms and functions. J. Comput. Neurosci. *1*, 11–38.

Hallock, H.L., Wang, A., and Griffin, A.L. (2016). Ventral midline thalamus is critical for hippocampal–prefrontal synchrony and spatial working memory. J. Neurosci. *36*, 8372–8389.

Hasselmo, M.E., Bodelón, C., and Wyble, B.P. (2002). A proposed function for hippocampal theta rhythm: separate phases of encoding and retrieval enhance reversal of prior learning. Neural Comput. *14*, 793–817.

Hoover, W.B., and Vertes, R.P. (2007). Anatomical analysis of afferent projections to the medial prefrontal cortex in the rat. Brain Struct. Funct. *212*, 149–179.

Hoover, W.B., and Vertes, R.P. (2012). Collateral projections from nucleus reuniens of thalamus to hippocampus and medial prefrontal cortex in the rat: a single and double retrograde fluorescent labeling study. Brain Struct. Funct. *217*, 191–209.

Horst, N.K., and Laubach, M. (2013). Reward-related activity in the medial prefrontal cortex is driven by consumption. Front. Neurosc. *7*, 56.

Hyman, J.M., Zilli, E.A., Paley, A.M., and Hasselmo, M.E. (2005). Medial prefrontal cortex cells show dynamic modulation with the hippocampal theta rhythm dependent on behavior. Hippocampus *15*, 739–749.

Hyman, J.M., Zilli, E.A., Paley, A.M., and Hasselmo, M.E. (2010). Working memory performance correlates with prefrontal-hippocampal theta interactions but not with prefrontal neuron firing rates. Front. Integr. Nuerosci. *4*, 2.

Hyman, J.M., Hasselmo, M.E., and Seamans, J.K. (2011). What is the functional relevance of prefrontal cortex entrainment to hippocampal theta rhythms? Front. Neurosci. *5*, 24.

Hyman, J.M., Ma, L., Balaguer-Ballester, E., Durstewitz, D., and Seamans, J.K. (2012). Contextual encoding by ensembles of medial prefrontal cortex neurons. Proc. Natl. Acad. Sci. U S A *109*, 5086–5091.

Hyman, J.M., Holroyd, C.B., and Seamans, J.K. (2017). A novel neural prediction error found in anterior cingulate cortex ensembles. Neuron *95*, 447–456.

Ito, H.T., Zhang, S.J., Witter, M.P., Moser, E.I., and Moser, M.B. (2015). A prefrontal-thalamo-hippocampal circuit for goal-directed spatial navigation. Nature *522*, 50–55.

Ito, H.T., Moser, E.I., and Moser, M.B. (2018). Supramammillary nucleus modulates spike-time coordination in the prefrontal-thalamo-hippocampal circuit during navigation. Neuron *99*, 576–587.e5.

Izaki, Y., Hori, K., and Nomura, M. (2000). Disturbance of rat lever-press learning by hippocampo-prefrontal disconnection. Brain Res. *860*, 199–202.

Jackson, J.C., Johnson, A., and Redish, A.D. (2006). Hippocampal sharp waves and reactivation during awake states depend on repeated sequential experience. J. Neurosci. *26*, 12415–12426.

Jones, M.W., and Wilson, M.A. (2005). Theta rhythms coordinate hippocampal-prefrontal interactions in a spatial memory task. PLoS Biol. *3*, e402.

Kay, S.M. (1988). Modern Spectral Estimation (Prentice Hall).

Kinsky, N.R., Sullivan, D.W., Mau, W., Hasselmo, M.E., and Eichenbaum, H.B. (2018). Hippocampal place fields maintain a coherent and flexible map across long timescales. Curr. Biol. *28*, 3578–3588.e6.

Kitamura, T., Ogawa, S.K., Roy, D.S., Okuyama, T., Morrissey, M.D., Smith, L.M., Redondo, R.L., and Tonegawa, S. (2017). Engrams and circuits crucial for systems consolidation of a memory. Science *356*, 73–78.

Kragel, J.E., Ezzyat, Y., Sperling, M.R., Gorniak, R., Worrell, G.A., Berry, B.M., Inman, C., Lin, J.J., Davis, K.A., Das, S.R., et al. (2017). Similar patterns of neural activity predict memory function during encoding and retrieval. Neuroimage *155*, 60–71.

Lee, I., and Kesner, R.P. (2003). Time-dependent relationship between the dorsal hippocampus and the prefrontal cortex in spatial memory. J. Neurosci. *23*, 1517–1523.

Lee, I., Griffin, A.L., Zilli, E.A., Eichenbaum, H., and Hasselmo, M.E. (2006). Gradual translocation of spatial correlates of neuronal firing in the hippocampus toward prospective reward locations. Neuron *51*, 639–650.

Linley, S.B., Gallo, M.M., and Vertes, R.P. (2016). Lesions of the ventral midline thalamus produce deficits in reversal learning and attention on an odor texture set shifting task. Brain Res. *1649* (*Pt A*), 110–122.

Lopes, G., Bonacchi, N., Frazão, J., Neto, J.P., Atallah, B.V., Soares, S., Moreira, L., Matias, S., Itskov, P.M., Correia, P.A., et al. (2015). Bonsai: an event-based framework for processing and controlling data streams. Front. Neuroinform. *9*, 7.

Ma, L., Hyman, J.M., Lindsay, A.J., Phillips, A.G., and Seamans, J.K. (2014). Differences in the emergent coding properties of cortical and striatal ensembles. Nat. Neurosci. *17*, 1100–1106.

Ma, L., Hyman, J.M., Durstewitz, D., Phillips, A.G., and Seamans, J.K. (2016). A quantitative analysis of context-dependent remapping of medial frontal cortex neurons and ensembles. J. Neurosci. *36*, 8258–8272.

Maviel, T., Durkin, T.P., Menzaghi, F., and Bontempi, B. (2004). Sites of neocortical reorganization critical for remote spatial memory. Science *305*, 96–99.

McClelland, J.L., McNaughton, B.L., and O'Reilly, R.C. (1995). Why there are complementary learning systems in the hippocampus and neocortex: insights from the successes and failures of connectionist models of learning and memory. Psychol. Rev. *102*, 419–457.

McGaugh, J.L. (2000). Memory–a century of consolidation. Science *287*, 248–251.

McKenzie, S., and Eichenbaum, H. (2011). Consolidation and reconsolidation: two lives of memories? Neuron *71*, 224–233.

McNaughton, N., and Sedgwick, E.M. (1978). Reticular stimulation and hippocampal theta rhythm in rats: effects of drugs. Neuroscience *3*, 629–632.

Mishkin, M. (1979). Analogous neural models for tactual and visual learning. Neuropsychologia *17*, 139–151.

Mishkin, M. (1982). A memory system in the monkey. Philos. Trans. R. Soc. Lond. B Biol. Sci. *298*, 83–95.

Muller, R.U., and Kubie, J.L. (1987). The effects of changes in the environment on the spatial firing of hippocampal complex-spike cells. J. Neurosci. *7*, 1951–1968.

Myroshnychenko, M., Seamans, J.K., Phillips, A.G., and Lapish, C.C. (2017). Temporal dynamics of hippocampal and medial prefrontal cortex interactions during the delay period of a working memory-guided foraging task. Cereb. Cortex *27*, 5331–5342.

O'Neill, P.K., Gordon, J.A., and Sigurdsson, T. (2013). Theta oscillations in the medial prefrontal cortex are modulated by spatial working memory and synchronize with the hippocampus through its ventral subregion. J. Neurosci. *33*, 14211–14224.

Onslow, A.C., Bogacz, R., and Jones, M.W. (2011). Quantifying phase-amplitude coupling in neuronal network oscillations. Prog. Biophys. Mol. Biol. *105*, 49–57.

Paus, T., Koski, L., Caramanos, Z., and Westbury, C. (1998). Regional differences in the effects of task difficulty and motor output on blood flow response in the human anterior cingulate cortex: a review of 107 PET activation studies. Neuroreport *9*, R37–R47.

Phelps, E.A., LaBar, K.S., Anderson, A.K., O'connor, K.J., Fulbright, R.K., and Spencer, D.D. (1998). Specifying the contributions of the human amygdala to emotional memory: a case study. Neurocase *4*, 527–540.

Pickenhain, L., and Klingberg, F. (1967). Hippocampal slow wave activity as a correlate of basic behavioral mechanisms in the rat. In Progress in Brain Research, W.R. Adey and T. Tokizane, eds. (Elsevier), pp. 218–227.

Piolino, P., Giffard-Quillon, G., Desgranges, B., Chételat, G., Baron, J.C., and Eustache, F. (2004). Re-experiencing old memories via hippocampus: a PET study of autobiographical memory. Neuroimage *22*, 1371–1383.

Place, R., Farovik, A., Brockmann, M., and Eichenbaum, H. (2016). Bidirectional prefrontal-hippocampal interactions support context-guided memory. Nat. Neurosci. *19*, 992–994.

Quillfeldt, J.A., Zanatta, M.S., Schmitz, P.K., Quevedo, J., Schaeffer, E., Lima, J.B., Medina, J.H., and Izquierdo, I. (1996). Different brain areas are involved in memory expression at different times from training. Neurobiol. Learn. Mem. *66*, 97–101.

Rajasethupathy, P., Sankaran, S., Marshel, J.H., Kim, C.K., Ferenczi, E., Lee, S.Y., Berndt, A., Ramakrishnan, C., Jaffe, A., Lo, M., et al. (2015). Projections from neocortex mediate top-down control of memory retrieval. Nature *526*, 653–659.

Restivo, L., Vetere, G., Bontempi, B., and Ammassari-Teule, M. (2009). The formation of recent and remote memory is associated with time-dependent formation of dendritic spines in the hippocampus and anterior cingulate cortex. J. Neurosci. *29*, 8206–8214.

Rissman, J., and Wagner, A.D. (2012). Distributed representations in memory: insights from functional brain imaging. Annu. Rev. Psychol. *63*, 101–128.

Rolls, E.T. (2000). The orbitofrontal cortex and reward. Cereb. Cortex *10*, 284–294.

Roy, A., Svensson, F.P., Mazeh, A., and Kocsis, B. (2017). Prefrontal-hippocampal coupling by theta rhythm and by 2-5 Hz oscillation in the delta band: the role of the nucleus reuniens of the thalamus. Brain Struct. Funct. *222*, 2819–2830.

Rozeske, R.R., Valerio, S., Chaudun, F., and Herry, C. (2015). Prefrontal neuronal circuits of contextual fear conditioning. Genes Brain Behav. *14*, 22–36.

Rugg, M.D., and Vilberg, K.L. (2013). Brain networks underlying episodic memory retrieval. Curr. Opin. Neurobiol. *23*, 255–260.

Scoville, W.B., and Milner, B. (1957). Loss of recent memory after bilateral hippocampal lesions. J. Neurol. Neurosurg. Psychiatry *20*, 11–21.

Sesack, S.R., Deutch, A.Y., Roth, R.H., and Bunney, B.S. (1989). Topographical organization of the efferent projections of the medial prefrontal cortex in the rat: an anterograde tract-tracing study with Phaseolus vulgaris leucoagglutinin. J. Comp. Neurol. *290*, 213–242.

Shidara, M., Mizuhiki, T., and Richmond, B.J. (2005). Neuronal firing in anterior cingulate neurons changes modes across trials in single states of multitrial reward schedules. Exp. Brain Res. *163*, 242–245.

Siapas, A.G., Lubenov, E.V., and Wilson, M.A. (2005). Prefrontal phase locking to hippocampal theta oscillations. Neuron *46*, 141–151.

Siegle, J.H., López, A.C., Patel, Y.A., Abramov, K., Ohayon, S., and Voigts, J. (2017). Open Ephys: an open-source, plugin-based platform for multichannel electrophysiology. J. Neural Eng. *14*, 045003.

Sigurdsson, T., Stark, K.L., Karayiorgou, M., Gogos, J.A., and Gordon, J.A. (2010). Impaired hippocampal-prefrontal synchrony in a genetic mouse model of schizophrenia. Nature *464*, 763–767.

Sinnamon, H.M., and Schwartzbaum, J.S. (1973). Dorsal hippocampal unit and egg responses to rewarding and aversive brain stimulation in rats. Brain Res. *56*, 183–202.

Sirota, A., Montgomery, S., Fujisawa, S., Isomura, Y., Zugaro, M., and Buzsáki, G. (2008). Entrainment of neocortical neurons and gamma oscillations by the hippocampal theta rhythm. Neuron *60*, 683–697.

Slotnick, B.M., Kufera, A., and Silberberg, A.M. (1991). Olfactory learning and odor memory in the rat. Physiol. Behav. *50*, 555–561.

Squire, L.R., and Alvarez, P. (1995). Retrograde amnesia and memory consolidation: a neurobiological perspective. Curr. Opin. Neurobiol. *5*, 169–177.

Squire, L.R., Schmolck, H., and Stark, S.M. (2001). Impaired auditory recognition memory in amnesic patients with medial temporal lobe lesions. Learn. Mem. *8*, 252–256.

Squire, L.R., Genzel, L., Wixted, J.T., and Morris, R.G. (2015). Memory consolidation. Cold Spring Harb. Perspect. Biol. *7*, a021766.

Steenland, H.W., Li, X.Y., and Zhuo, M. (2012). Predicting aversive events and terminating fear in the mouse anterior cingulate cortex during trace fear conditioning. J. Neurosci. *32*, 1082–1095.

Stephens, M.A. (1969). Tests for randomness of directions against two circular alternatives. J. Am. Stat. Assoc. *64*, 280–289.

Suzuki, A., Josselyn, S.A., Frankland, P.W., Masushige, S., Silva, A.J., and Kida, S. (2004). Memory reconsolidation and extinction have distinct temporal and biochemical signatures. J. Neurosci. *24*, 4787–4795.

Takehara, K., Kawahara, S., and Kirino, Y. (2003). Time-dependent reorganization of the brain components underlying memory retention in trace eyeblink conditioning. J. Neurosci. *23*, 9897–9905.

Takehara-Nishiuchi, K., and McNaughton, B.L. (2008). Spontaneous changes of neocortical code for associative memory during consolidation. Science *322*, 960–963.

Tamura, M., Spellman, T.J., Rosen, A.M., Gogos, J.A., and Gordon, J.A. (2017). Hippocampal-prefrontal theta-gamma coupling during performance of a spatial working memory task. Nat. Commun. *8*, 2182.

Teixeira, C.M., Pomedli, S.R., Maei, H.R., Kee, N., and Frankland, P.W. (2006). Involvement of the anterior cingulate cortex in the expression of remote spatial memory. J. Neurosci. *26*, 7555–7564.

Thompson, L.T., and Best, P.J. (1990). Long-term stability of the place-field activity of single units recorded from the dorsal hippocampus of freely behaving rats. Brain Res. *509*, 299–308.

Tort, A.B., Komorowski, R.W., Manns, J.R., Kopell, N.J., and Eichenbaum, H. (2009). Theta-gamma coupling increases during the learning of item-context associations. Proc. Natl. Acad. Sci. U S A *106*, 20942–20947.

Vanderwolf, C.H. (1969). Hippocampal electrical activity and voluntary movement in the rat. Electroencephalogr. Clin. Neurophysiol. *26*, 407–418.

Vanderwolf, C.H., Bland, B.H., and Whishaw, I.Q. (1973). Diencephalic, hippocampal, and neocortical mechanisms in voluntary movement. In Efferent Organization and the Integration of Behavior, J.D. Maser, ed. (Academic Press).

Varela, C., Kumar, S., Yang, J.Y., and Wilson, M.A. (2014). Anatomical substrates for direct interactions between hippocampus, medial prefrontal cortex, and the thalamic nucleus reuniens. Brain Struct. Funct. *219*, 911–929.

Varela, C., Weiss, S., Meyer, R., Halassa, M., Biedenkapp, J., Wilson, M.A., Goosens, K.A., and Bendor, D. (2016). Tracking the time-dependent role of the hippocampus in memory recall using DREADDs. PLoS ONE *11*, e0154374.

Vertes, R.P. (2002). Analysis of projections from the medial prefrontal cortex to the thalamus in the rat, with emphasis on nucleus reuniens. J. Comp. Neurol. *442*, 163–187.

Vertes, R.P. (2006). Interactions among the medial prefrontal cortex, hippocampus and midline thalamus in emotional and cognitive processing in the rat. Neuroscience *142*, 1–20.

Vertes, R.P., and Kocsis, B. (1994). Projections of the dorsal raphe nucleus to the brainstem: PHA-L analysis in the rat. J. Comp. Neurol. *340*, 11–26.

Vetere, G., Restivo, L., Cole, C.J., Ross, P.J., Ammassari-Teule, M., Josselyn, S.A., and Frankland, P.W. (2011). Spine growth in the anterior cingulate cortex is necessary for the consolidation of contextual fear memory. Proc. Natl. Acad. Sci. U S A *108*, 8456–8460.

Viard, A., Piolino, P., Desgranges, B., Chételat, G., Lebreton, K., Landeau, B., Young, A., De La Sayette, V., and Eustache, F. (2007). Hippocampal activation for autobiographical memories over the entire lifetime in healthy aged subjects: an fMRI study. Cereb. Cortex *17*, 2453–2467.

Viard, A., Lebreton, K., Chételat, G., Desgranges, B., Landeau, B., Young, A., De La Sayette, V., Eustache, F., and Piolino, P. (2010). Patterns of hippocampal-neocortical interactions in the retrieval of episodic autobiographical memories across the entire life-span of aged adults. Hippocampus *20*, 153–165.

Viena, T.D., Linley, S.B., and Vertes, R.P. (2018). Inactivation of nucleus reuniens impairs spatial working memory and behavioral flexibility in the rat. Hippocampus *28*, 297–311.

Walton, M.E., and Mars, R.B. (2007). Probing human and monkey anterior cingulate cortex in variable environments. Cogn. Affect. Behav. Neurosci. *7*, 413–422.

Wang, G.W., and Cai, J.X. (2008). Reversible disconnection of the hippocampal-prelimbic cortical circuit impairs spatial learning but not passive avoidance learning in rats. Neurobiol. Learn. Mem. *90*, 365–373.

Weible, A.P., Rowland, D.C., Pang, R., and Kentros, C. (2009). Neural correlates of novel object and novel location recognition behavior in the mouse anterior cingulate cortex. J. Neurophysiol. *102*, 2055–2068.

Weible, A.P., Rowland, D.C., Monaghan, C.K., Wolfgang, N.T., and Kentros, C.G. (2012). Neural correlates of long-term object memory in the mouse anterior cingulate cortex. J. Neurosci. *32*, 5598–5608.

Westendorff, S., Kaping, D., Everling, S., and Womelsdorf, T. (2016). Prefrontal and anterior cingulate cortex neurons encode attentional targets even when they do not apparently bias behavior. J. Neurophysiol. *116*, 796–811.

Wilson, M.A., and McNaughton, B.L. (1993). Dynamics of the hippocampal ensemble code for space. Science *261*, 1055–1058.

Wiltgen, B.J., Zhou, M., Cai, Y., Balaji, J., Karlsson, M.G., Parivash, S.N., Li, W., and Silva, A.J. (2010). The hippocampus plays a selective role in the retrieval of detailed contextual memories. Curr. Biol. *20*, 1336–1344.

Wirt, R.A., and Hyman, J.M. (2017). Integrating spatial working memory and remote memory: interactions between the medial prefrontal cortex and hippocampus. Brain Sci. *7*, 43.

Witter, M.P., Wouterlood, F.G., Naber, P.A., and Van Haeften, T. (2000). Anatomical organization of the parahippocampal-hippocampal network. Ann. N.Y. Acad. Sci. *911*, 1–24.

STAR★METHODS

KEY RESOURCES TABLE

REAGENT or RESOURCE	SOURCE	IDENTIFIER
Bacterial and Virus Strains		
Biological Samples		n/a
Experimental Models: Organisms/Strains		
Long-Evans	Charles River Labs	n/a
Software and Algorithms		
Open Ephys	Siegle et al., 2017	http://www.open-ephys.org/
Bonsai	Lopes et al., 2015	https://bonsai-rx.org/
EEGLAB	Delorme and Makeig, 2004	https://sccn.ucsd.edu/eeglab/download.php
MV_GC	Barnett and Seth, 2014	https://users.sussex.ac.uk/~lionelb/MVGC/
MATLAB	Mathworks	n/a
Plexon offline sorter	Plexon	n/a
Other		
Intan	Intan technologies	n/a

CONTACT FOR REAGENT AND RESOURCE SHARING

Further information and requests for resources and reagents should be directed to and will be fulfilled by the Lead Contact, James M. Hyman (james.hyman@unlv.edu).

EXPERIMENTAL MODEL AND SUBJECT DETAILS

Seven male Long-Evans rats (8-12 months) obtained from Charles River Laboratories, Inc. (Wilmington, MA) were used in this experiment. Subjects were given a minimum of three days after arrival prior to any experimental procedures, after this time, subjects were handled by experimenters for a minimum of two weeks before surgery. After surgery, subjects were individually housed on a twelve-hour light-dark cycle with food and water available *ad libitum*. All experimental procedures took place during the light cycle and were approved by the University of Nevada Las Vegas Institutional Animal Care and Use Committee.

METHOD DETAILS

Surgery and Electrophysiology

Subjects were deeply anesthetized using isoflurane gas (1 – 3%) and implanted with 32 movable tetrodes in a hyperdrive affixed to the animal's skull. 16 tetrodes targeted bilateral ACC (2.5 mm anterior; + 0.5 lateral; 8 left and 8 right), and 16 tetrodes targeted bilateral dorsal CA1 (3.5 mm posterior to bregma; + 2.5 lateral; 8 left and 8 right). Two posterior screws placed just above the cerebellum were connected to a grounding wire and soldered into the electrode interface board (EIB; Plexon Inc. Dallas, Texas) as is typically done in rodent *in vivo* recordings (Buzsáki, 1986). After the tetrodes were positioned over the targeted brain areas, we affixed it to the skull using dental acrylic. When the dental acrylic had fully hardened, the tetrodes were lowered 400 μm into the cortex. After a 7 day recovery period we slowly lowered tetrodes ventrally into the ACC (~2.5 mm) and the pyramidal cell layer of dorsal CA1 using electrophysiological markers (Buzsáki, 1986).

Electrodes were connected to a 128 channel EIB which plugged into four headstages (Intan Technologies, Los Angeles, CA). Digitized electrophysiological signals were sent up tether cables into the into the RHD 2000 USB interface board (Intan Technologies, Los Angeles, CA) which feeds the digital signal into a computer workstation. Electrophysiological data was read into Open Ephys (Cambridge, MA). Data was acquired at a sampling rate of 30 KHz. During acquisition continuous data were bandpass filtered between 1-6000 Hz and spike data were bandpass filtered between 600-6000 Hz. Spike data was then read into Offline Sorter (Plexon Inc.) for spike sorting using 2D and 3D projections to discern visually dissociable clusters. Spike timestamps were then read into MATLAB (Mathworks, Natick, Massachusetts) for further analyses.

Behavior

Subjects were placed into a series of environments situated in the center of a lowly lit room. Throughout the experiment, subjects were exposed to seven unique environments all with high walls (> 22 inches) to limit influences from distal recording room cues.

All environments were distinct in size, shape, texture, and visual stimuli present. Each environment was made of a different material (corrugated plastic, polyethylene, cardboard, vinyl, PVC, laminated poster board) or a unique combination of these materials, which created a texture contrast between environments. An array of visual cues (varying by color and shape) were on the walls of each environment. Each environment was placed in the same location within the recording room. For each session, animals were brought to the recording room and allowed to habituate for a minimum of thirty minutes. After that time, subjects were placed on a pedestal and fed Froot Loops (Kellogg's, Battle Creek, MI) while the headstages were plugged into the EIB. When the connection was secured, animals were placed into an environment and allowed to freely explore for exactly ten minutes. After this time, subjects were removed from the environment and placed upon the pedestal for one minute before being placed into the next environment. See Figure 1A for a schematic breakdown of environment exposures. Briefly, during session one (RI-0), subjects were introduced to environment A and B. Session two (RI-1), subjects re-explored environment A and then were introduced into environments C and D. On session three (RI-2), subjects were re-exposed to environments B and D and then introduced to environment E. Session four was a reset day (RD) and used to control for differences in time from last visit before our remote recall sessions and no electrophysiological recordings took place on this day though subjects were attached to the recording tether. During this session, subjects were re-exposed to environments A, B, C, D, and E, and also introduced to environment F. Session five took place seven days after session four (RI-7) and subjects were reintroduced into environments A, C, and E. Fourteen days after the fourth session (RI-14), subjects were reintroduced into environments B, D, and F, and introduced to environment G (see Figure 1A). These intervals were chosen based upon previous studies that showed remote recall effects in ACC after similar delays (Takehara-Nishiuchi and McNaughton, 2008). For example, Frankland et al. (2004) found memory deficits with ACC inactivation at 2 weeks and 5 weeks, but no effects at 1 or 3 days. Concurrently, Suzuki et al. (2004) found delivery of anisomycin, preventing reconsolidation, caused subsequent memory impairments if the re-exposure and anisomycin delivery took place 1 week after learning. Similar results were found for 3 and 6 weeks, suggesting that the memory had been consolidated after the one week interval.

The order of environments was constructed so that later analyses could be performed on two consecutive environments or dyads. This order allowed us to counterbalance the number of novel-novel, novel-familiar, and familiar-familiar environment dyads. Each animal was exposed to the same sequence of environments to control for any possible order effects. Given that this experiment featured seven subjects and seven unique environments, proper environmental counterbalancing would require each animal to have experienced a unique sequence, which would have introduced lots of possible variance. Thus, we chose to use the same order in all animals and believe that the risk of order effects corrupting our sample was low. Video and path data were gathered using Bonsai behavioral tracking software.

Histology

After subjects completed the experiment, they were deeply anesthetized under isoflurane gas and electrolytic lesions were created by passing current through all ACC and hippocampal wires. Subjects were then perfused with a solution containing 250 mL 10% buffered formalin, 10 mL glacial acetic acid, and 10 g of potassium ferrocyanide. The brains were removed and stored in a solution containing 10% buffered formalin and sucrose for a minimum of 1 week. After that time, brains were sliced at 40 μm and mounted on slides for visual inspection of wire tracks (see Figures 1B and 1C).

QUANTIFICATION AND STATISTICAL ANALYSIS

Behavioral Analysis

To quantify behavioral changes that occurred due to re-exposure of environments, we examined distance traveled and the amount of time spent in the center areas of each environment. To examine gross locomotor activity, we calculated the total distance traveled over each exposure in one-minute time bins. Since each environment was unique in shape, size, and texture, all of which could affect total distance traveled, and during each session animals only visited 3 out 6 environments, we needed to control for variance between environments. We first grouped the raw values from each environment, combining all retention intervals and subjects, and then z-transformed these populations. This allowed us to isolate any variance in distance traveled based upon amount of time in an environment and amount time since the environment was last visited. To test recall effects of re-exposure to environments we calculated the percent of time animals spent in the center (half the total area) relative to the periphery of the environment (inside/outside). Environment A was in the shape of a triangle and had a total area of 444 cm. Environment B was hexagonal shaped and had a total area of 1600 cm. Environment C was circular and had a total area of 650 cm. Environment D was diamond shaped and had a total area of 1200 cm. Environment E was square and had a total area of 1400 cm. Environment F was rectangular and had a total area of 1100 cm. Environment G was "V" shaped and had a total area of 850 cm.

Using custom written MATLAB code, each environment was separated into a set of standardized squares, we then calculated the percent of time spent in each square compared to all other squares during environment exposure. As an additional measure of memory recall, we calculated time spent computed as:

$$P = \frac{T_n}{(\Sigma(\Sigma T_n))}$$

where P is the percent time spent, T overall time spent, and *n* is each separated location, of the 120 s time window. This allowed us to evaluate the extent of exploratory behavior in the entire environment. To do this, we calculated the cumulative sum using the MATLAB function *cumsum* and corresponding definite integral (area under the curve or AUC) using the MATLAB function *trapz* of the standardized squares in each environment. We then performed a one-way ANOVA to compare AUC values over retention intervals.

Analysis of Continuous Data

After experimental procedures concluded, data were read into a computer workstation and down sampled to 1000 Hz using custom written MATLAB code. To remove the 60 Hz noise signal, data were notch filtered between 58 and 61 Hz using MATLAB function *butter*. Next, we identified "good wires' through visual inspection to minimize signal redundancy, leaving four per recording area but only one from any single tetrode. For all comparisons each exposure was treated individually, so during each recording session exposures could contribute to data groups according to retention interval. For example, in session 3 animals were first re-exposed to environment B (2 day retention interval), next they were re-exposed to environment D (1 day retention interval), and last they were exposed to environment E (initial exposure or 0 day retention interval).

Coherence

To test how oscillatory activity changed between the ACC and CA1 over recording days, we calculated coherence during exposures to each environment for all recording sessions. We used the MATLAB function *mscohere* on notch filtered LFPs. The coherence value is computed as

$$C_{xy}(f) = \frac{\left|P_{xy}(f)\right|^2}{P_{xx}(f)P_{yy}(f)}$$

where C is the coherence value between 0 and 1, P is power spectral densities, x and y are respective signals, and *f* is frequency (Kay, 1988). We calculated theta coherence between ACC and CA1 recording sites for all 8 ipsilateral pairs of LFP signals per environment exposure (see Figure 3A). We then normalized values in the theta range (7-12 Hz) by z-transformation (MATLAB function *zscore*) of data groups by environment. This helped to eliminate any differences due to size or shape of environments from affecting our comparisons as done above. A single factor ANOVA was used to compare coherence values during each recording session. To examine signal power, a Fast Fourier transform (FFT) was computed using the MATLAB function *fft.* Results from ACC and hippocampal FFT were analyzed separately. Values in the theta range were then normalized for each environment and examined across each delay period using and one-way ANOVA.

Granger Prediction

To assess directionality of LFP interactions we used a frequency resolved measure of Granger prediction, provided by a freely available MATLAB toolbox (*MVGC: multivariate Granger causality toolbox*; Barnett and Seth, 2014). This method examines how predictive one signal is of another. First, higher order autoregressive models were created for each pair of ipsilateral ACC-CA1 leads for each exposure. 60Hz notch-filtered high sampling rate data was binned in 1 s bins for the first 120 s of environment exposure. The data were tested for stability over time and the model order was chosen by Bayesian information criterion. These values were then spectrally resolved according to Geweke's formulation (Geweke, 1982). Mean Granger prediction values within the theta range (7-12Hz) were then compared across conditions.

Theta-Gamma Cross Frequency Phase-Amplitude Coupling

Phase to amplitude coupling techniques were first described by Tort et al. (2009). For this analysis, we examined the modulation index (MI) or the rate at which the amplitude of gamma band LFPs from either CA1 or ACC were influenced by the theta phase of LFPs in the other area. MI values are between 0 and 1 and were generated using the freely available *Neurodynamics Lab* MATLAB toolbox function *ModIndex_v2*. Changes in MI by retention interval were examined using a one-way ANOVA.

Analysis of Unit Data

After each recording session spike data were read into a computer work station and translated into (*.nex*) format using custom written MATLAB code. Single unit data were sorted based off of waveform characteristics using Plexon Offline Sorting (Plexon Inc, Dallas, TX). Spiking data were then read into MATLAB for further analysis. In addition to examining oscillatory interactions between the ACC and CA1, we also were interested in understanding how theta activity affected unit firing.

Unit Theta Phase-Locking

For each cell we calculated the degree of theta entrainment to all 4 ipsilateral leads in the other area during the initial period in each environment and looked at the maximum value from all comparisons. To analyze phasic modulation of unit spike trains we first Hilbert transformed the theta range filtered LFPs to extract instantaneous phase using the MATLAB function *hilbert*. A cell was considered modulated based off of the distribution of spike times relative to theta oscillations. We found the phase for each spike during the first

120 s in each environment and used Rayleigh's test of uniformity to assess whether a cell was significantly modulated. The Rayleigh test statistic is computed as

$$Z = nR^2$$

where n equals the number of spikes and R the mean resultant length (or the magnitude of the vector that results when each spike is represented as a vector on the unit circle whose angle relative to some fixed point is given by the spike's phase and the vectors are all summed together) (Stephens, 1969; Hyman et al., 2005). We performed ANOVAs that compared ACC or CA1 unit MRL by retention interval, and also compared percentage of ACC or CA1 units that were phase-locked to the other area's theta oscillations for each retention interval. Note that some cells could be counted in multiple categories, however, entrainment was only considered by individual environment exposure, so a cell recorded during session 2 contributed to both retention interval day 0 and day 1 counts.

Mahalanobis Distance

To examine how ensemble activity states differed between environments we employed an analytical approach similar to our previous work (Hyman et al., 2012). Our experimental setup was designed so animals would be presented with novel environments following both day 1 and day 2 recall exposures, allowing us to expose the animals to many environments over days and also helping to minimize potential memory interference effects within sessions. However, since this analysis required comparisons of two environmental contexts at a time, we thus needed to control for an animal's familiarity with both environments, while also isolating any changes that occurred due to retention interval length. To this end we grouped comparisons together based on level of familiarity with both environments and retention interval of one or both environments. Our first step was to group the cells based upon recording session, which allowed us to compare based upon either familiarity or retention interval.

Neural firing rates were estimated for each isolated cell as a function of time binning (500ms). This relatively long time bin size is ideal for examining contextual representations, which should be reflected in the steady state firing rates and thus less sensitive to transient behavioral changes. 500ms time bins were also used in our previous paper analyzing contextual representations across ACC and CA1 ensembles (Hyman et al., 2012). Cells with fewer than 50 spikes during the behaviorally relevant period were excluded from analysis. To control for differences in recorded ensemble size (mean ensemble size = 41 cells; range = 8-120) and any momentary behavioral differences that occurred between sessions, we normalized the number of cells considered for both areas. We randomly drew 40 cell ACC and CA1 ensembles for each recording session type. To determine ensemble activity states between contexts, we normalized each unit's firing rate and then randomly selected 1000 CA1 and ACC ensembles for each session type, leaving 5000 CA1 and 5000 ACC ensembles. We computed dMah in the full high dimensional MSUA space between the first 120 s (240 time points) of each exposure. Principal components were only used for the 3D visualizations of MSUA state spaces shown in Figure 5B.

Each environment was classified as either novel (initial exposure only) or familiar (any subsequent exposure). This left us with three types of comparisons: novel versus novel (NN), familiar versus novel (FN), or familiar versus familiar (FF). These were spread relatively evenly over the recording sessions.

Selectivity Index

A selectivity index for each unit was constructed to identify if it exhibited preference for one environment over another. Thus, for this analysis cells were grouped by the type of environment exposure as described above for the dMah analysis. The selectivity index, previously described in (Hyman et al., 2012; Ma et al., 2014), was obtained by grouping firing rates of neuron i during each environment exposure. The index was computed as

$$d_i' = \frac{|\langle \{r_i(t) \mid t \in E_n\} - r_i(t) | t \in E_{n+1} \rangle|}{\sqrt{\sigma_i^2 t \in E_n + \sigma_i^2 t \in E_{n+1}}}$$

where $\langle\ \rangle$ denotes the mean.

DATA AND SOFTWARE AVAILABILITY

Analysis-specific code and datasets are available by request to the Lead Contact: james.hyman@unlv.edu